Chemical Engineering Journal 500 (2024) 157222

Contents lists available at ScienceDirect

Chemical Engineering Journal

journal homepage: www.elsevier.com/locate/cej

Review

Electrochemical advanced oxidation of per- and polyfluoroalkyl substances (PFASs): Development, challenges and perspectives

Xiaoyong Xu [a,*], Yang Li [a], Phong H.N. Vo [b], Pradeep Shukla [c], Lei Ge [d], Chun-Xia Zhao [a]

[a] School of Chemical Engineering, The University of Adelaide, Adelaide, SA 5005, Australia
[b] Climate Change Cluster, Faculty of Science, University of Technology Sydney, 15 Broadway, Ultimo, NSW 2007, Australia
[c] School of Chemical Engineering, The University of Queensland, Brisbane 4072, QLD, Australia
[d] School of Engineering, University of Southern Queensland, Springfield, QLD 4300, Australia

ARTICLE INFO

Keywords:
EAOPs
Per- and polyfluoroalkyl substances (PFASs)
Anode materials
Hydroxyl radical

ABSTRACT

Perfluoroalkyl and polyfluoroalkyl substances (PFAS) have been globally distributed since 1940, resulting in their widespread existence in natural environments. This is due to the remarkable stability of carbon–fluorine bonds, which are difficult to degrade chemically in a natural setting. PFASs accumulate in the human body through daily consumption of water and food, which can lead to potential health effects such as immune, metabolic, and neurodevelopmental effects. As a result, there is a growing global concern regarding PFAS remediation, given their toxicity and bio-accumulative properties in recent years. Electrochemical advanced oxidation processes (EAOPs) have been developed for the remediation of PFASs and have been applied in wastewater treatment. In these processes, a highly powerful oxidizing agent, hydroxyl radical ((•)OH), is generated electrochemically in solution, which can oxidize organic contaminants. EAOPs have become an environmentally friendly and effective treatment process for destroying PFASs. However, their slow reaction rate, poor performance stability, high energy consumption, and electrode erosion hinder their commercialization for water treatment. This paper provides a comprehensive overview of state-of-the-art anode materials and their corresponding degradation efficiency of PFASs through electrochemical remediation, along with future recommendations. A worldwide perspective on the fundamentals and experimental setups is provided, examining, and discussing different anode electrodes, as well as the challenges of EAOPs for PFAS remediation.

1. Introduction

Per- and polyfluoroalkyl substances (PFASs) are a group of man-made fluorinated compounds that have multiple fluorine atoms attached to an alkyl chain. A typical PFAS structure consists of a fluorinated hydrophobic “tail” and a hydrophilic “head,” making them suitable for use as surfactants. To date, ~15,000 different PFASs have been developed and are available in the market [1]. PFASs have been widely used in the manufacturing of extinguishers, surfactants, detergents, lubricants, paper, carpets, cosmetics, and aqueous film-forming foams (AFFFs) for firefighting since the 1950s. It is estimated that the total global release of PFASs from various sources (both direct and indirect) has been approximately 3200 to 7300 tons from 1940 to 2004 [2]. Due to the strong C–F bond and unique structure, PFASs possess great chemical and thermal stability, as well as superior surface-tension-lowering properties. Therefore, PFASs are resistant to natural chemical and biological degradation [3]. After years of being used in the market, PFASs have found their way into the ecosystem, and have the ability to accumulate in the human body.

There has been significant global attention on sulfonate and carboxylate PFAS forms, such as perfluorooctanoic acid (PFOA) and perfluorooctane sulfonic acid (PFOS), due to their potential adverse human health effects [4]. As a result of their environmental persistence, bioaccumulation, and toxicity, PFOA and PFOS pose potential risks to the ecosystem, especially to marine life [5]. PFASs have high mobility and can travel miles from the original release location, potentially leading to the formation of large plumes [6]. These compounds have been detected not only in groundwater but also in landfills worldwide [7]. The U.S. Centers for Disease Control and Prevention (CDC) has reported that PFASs are present in the blood of 98 % of the American population [8,9]. Epidemiology studies have linked PFAS exposure to tumors, cancer, and other adverse effects on public health. In recent

* Corresponding author.
E-mail address: xiaoyong.xu@adelaide.edu.au (X. Xu).

https://doi.org/10.1016/j.cej.2024.157222
Received 14 August 2024; Received in revised form 8 October 2024; Accepted 28 October 2024
Available online 30 October 2024

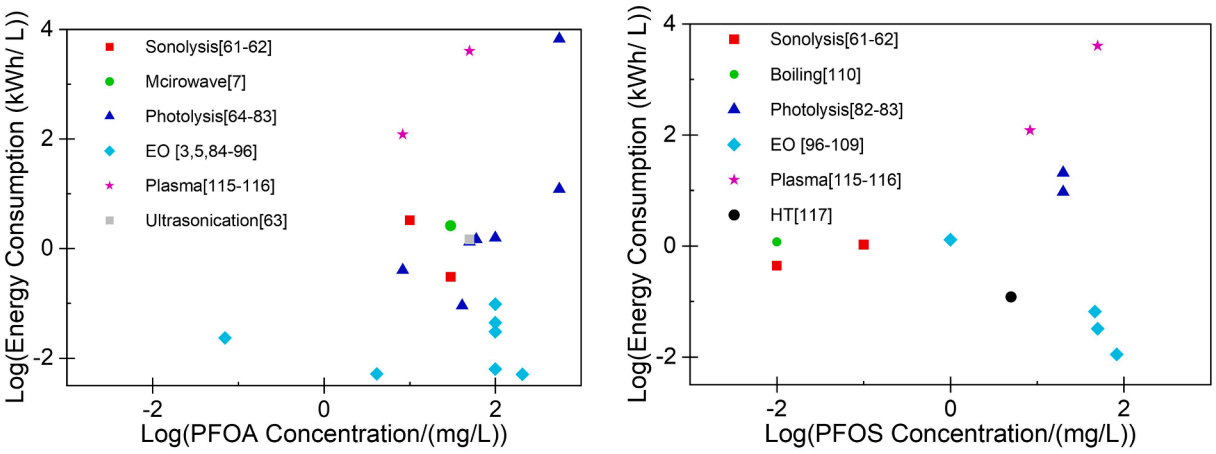

Fig. 1. Energy Consumption of PFAS destruction a) PFOA; b) PFOS.

Table 1
Potential of Oxygen Evolution Reaction on Different anodes in H_2SO_4 [133].

Anode	Class	Value vs SHE	Concentration of H_2SO_4
RuO_2	1	1.47	0.5 M
IrO_2	1	1.52	0.5 M
Pt	1	1.6	0.5 M
Graphite	1	1.7	0.5 M
SnO_2	2	1.9	0.05 M
PbO_2	2	1.9	1 M
BDD	2	2.3	0.5 M

Note: Standard Potential for Oxygen Evolution is 1.23 V vs SHE.

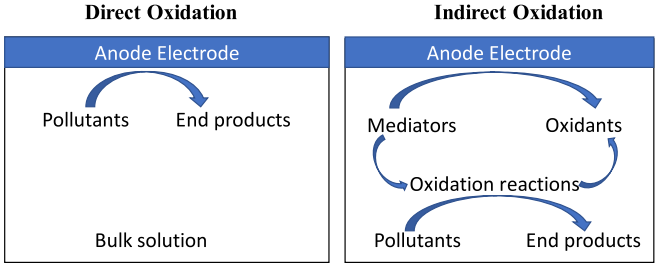

Fig. 2. Pathway of direct and indirect oxidation in anodic condition.

years, the growing concerns related to PFASs have drawn public attention as these compounds have been regulated in daily drinking water intake and the U.S. EPA recently issued a new National Primary Drinking Water Rule (NPDWR) on April 10, 2024, targeting six PFAS compounds. This rule establishes legally binding Maximum Contaminant Levels for PFOA, PFOS, PFHxS, PFNA, and HFPO-DA. Additionally, the rule introduces Hazard Indexes for assessing the combined risk of mixtures containing two or more of the following PFAS: PFNA, PFHxS, HFPO-DA, and PFBS [10]. Both surface water and groundwater are essential sources of drinking water. Over the past few decades, PFAS concentrations in surface water and groundwater have been found at ppt levels [11]. It has been widely recognized that dietary intake is the largest source of PFAS exposure [12–20]. The daily intake of drinking water, particularly in areas near industrial sites, is a significant source of PFASs exposure in human populations [21–25]. Daily food intake has also been identified as a dominant exposure pathway, as well as contact with PFASs-contaminated air and dust indoors through inhalation (up to 50 % of total PFASs intake) [26]. Populations who consume seafood frequently have reported elevated PFASs concentrations in their blood [27]. According to the European Food Safety Authority (EFSA), the primary chronic exposure to PFOA is through dairy products for babies, drinking water for infants, and seafood products for the elderly, accounting for up to 86 %, 60 %, and 56 % of total exposure, respectively [21].

Previous studies have provided strong evidence linking increased cancer risk with PFAS exposure and shown a positive correlation between PFOA levels and kidney and testicular cancers [22,28]. While Eriksen et al. [17] reported that it is not yet clear whether liver, bladder, pancreatic or prostate cancer are related to PFOA or PFOS concentrations, the International Agency for Research on Cancer (IARC) has classified PFOA as a possible human carcinogen, while no current evaluation is available for PFOS [21].

The risks associated with PFASs have highlighted the urgent need for effective treatment technology. According to a recent report from Bluefield Research [29], more than $3 billion is expected to be spent annually on drinking water remediation technologies by 2030, and the exponential increase of PFAS-related research underscores the growing interest in PFAS remediation.

Current treatment technologies for complete PFAS defluorination involve two main stages: concentration/separation and destruction. Most concentration/separation technologies immobilize PFASs into solid sorbents such as activated carbon [30–47], inorganic sorbents like resins [32,35,41–43,48–50], and clay or nano materials [44,51–60] which are then stabilized and stored in secure landfills. However, this technology has a significant drawback as PFASs are not defluorinated but merely relocated, leaving the risk of leaching intact. Additionally, there are other issues such as generating large volumes of waste for disposal, transferring contaminant risks on public roads and through populated areas, and requiring long-term maintenance and monitoring. Thus, a destruction technology is required in the separation step that can completely defluorinate PFASs into harmless end products.

Destruction technologies can defluorinate PFASs into innocuous end products using either chemicals, energy, or a combination of both to break the strong bond between carbon and fluorine. Current technologies for PFASs destruction include sonolysis [61,62], microwave [7], ultrasonication [63], photolysis [64–83], electrochemistry advanced oxidation process [3,5,84–109], boiling [110], high energy E-beam [111–113], high temperature steam [114], plasma [115,116], hydrothermal treatment (HT)[117] and supercritical water oxidation process (SCWO)[118]. The PFASs destruction technologies are known to consume significant amounts of energy. Therefore, they are preferably used to target highly concentrated, low-volume waste by reverse osmosis, membrane separation [119–124] and foam fractionation [125–127]. The energy consumption of PFOS and PFOA destruction by these technologies is summarized and presented in Fig. 1a-b. Among them, EAOP has not only the advantage in energy efficiency, but also other ones like less requirement on equipment, operation at ambient conditions etc. There is not enough data to calculate the energy

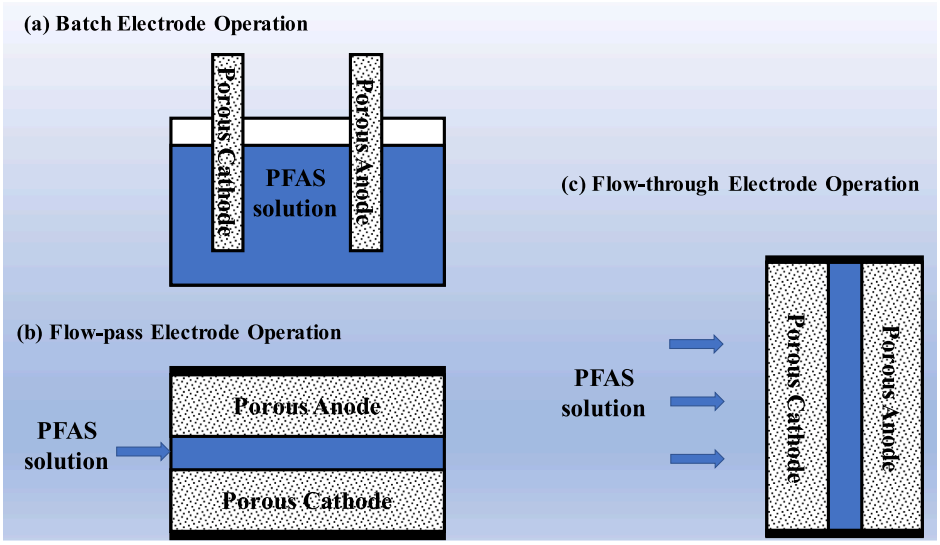

Fig. 3. Setup of Electrode operations: (a) batch electrode operation; (b) flow-pass electrode operation; (c) flow-through electrode operation.

consumption of PFAS destruction by E-beam [111–113]. Ma et al. [111] found that the degradation of PFOA and PFOS followed pseudo-first-order kinetics. In a nitrogen atmosphere, at a dose of 500 kGy (0.139 kWh/L) and a pH of 13, PFOA and PFOS degradation rates reached 95.7 % and 85.9 %, respectively. The defluorination rates were 46.8 % and 71.4 %, respectively. These results indicate that electron beam (EB) irradiation can effectively decompose PFOA and PFOS in anoxic alkaline solutions. No exact energy consumption was found for PFASs destruction by SCWO. It is reported that the SCWO system can achieve energy self-sufficiency when the chemical oxygen demand (COD) concentration exceeds 60,000 mg/L [118].

Recent review papers on the treatment of PFASs using EAOP have focused on past research and provided cumulative information on the topic, as well as the scope for future research [89,90,128–130]. However, to the best of our knowledge, there has been little research done on electrode materials and their design in order to improve degradation rates and stability performance. The objective of this review is to compare the performance of different anode materials and provide an overview of the feasibility and profitability of PFAS remediation through EAOP. While the cathode process is less investigated than the anode process, it can play an important role in wastewater treatment. In the EAOP of PFASs, PFASs decompose at the anode electrode, so the details of the cathode will not be discussed in this review. Thus, this review aims to: (1) provide an overview of the anode materials and their relevant working conditions; (2) assess the most effective anode materials and how material properties affect the remediation efficiency of EAOP; (3) study the reaction pathway of PFASs degradation through EAOP; and (4) discuss the challenges of EAOP for PFAS remediation.

2. PFAS electrochemical advanced oxidation processes

2.1. Fundamentals of EAOP

The advanced oxidation process (AOP) has gained popularity as a technology for treating organic or inorganic compounds in contaminated water in recent decades. Typically, hydroxyl radicals are utilized in AOP to attack and degrade the contaminants into non-toxic end products. Hydroxyl radicals, as one of the most aggressive oxidants, can be produced by employing ozone (O_3), hydrogen peroxide (H_2O_2) or UV light with catalysis. The lifetime of hydroxyl radicals is short, only 2 ~ 4 μs, and the possible contamination by the radicals is negligible, making it a popular option for wastewater treatment [75]. However, AOP usually requires harsh conditions and consumes a lot of chemicals or energy to produce hydroxyl radicals.

The electrochemical advanced oxidation process (EAOP) offers a promising solution for treating industrial wastewater. Unlike traditional methods that rely on UV or chemicals to produce hydroxyl radicals, EAOP utilizes electrochemistry to generate them as needed. This makes it a more environmentally friendly technology than conventional AOPs. EAOP can effectively eliminate a wide range of contaminants, such as PFASs [128] and other emerging contaminates [131], from wastewater, without generating waste that requires special handling. Compared to other technologies like adsorption, membrane, and anion exchange, EAOP offers a more sustainable alternative [132]. Pollutants in wastewater can be destroyed through direct or indirect electrolysis. Direct electrolysis occurs when the process is operated at low potentials, and pollutants are degraded on the anode surface without the involvement of other substances. EAOP of phenol is an example of direct electrolysis [133]. On the other hand, if the process is operated at high anodic overpotential, radicals with strong oxidizing and nonselective abilities are produced, including •OH, O_2^-•, SO_4^-• and CO_3^-•. These radicals can decompose some persistent pollutants, and we refer to this process as indirect electrolysis. EAOP of PFASs is an example of indirect electrolysis. It has been reported that the degradation of some PFASs (such as PFOS) by EAOP involves direct electron transfer and hydroxyl radicals. It is also believed that hydroxyl radicals alone cannot effectively degrade PFOS [134,135]. Therefore, the synergistic effect of direct electron transfer and hydroxyl radicals makes EAOP an effective PFAS degradation technology.

EAOP that occurs on the surface of electrodes is a surface-controlled process, mainly happening close to the electrode surface. As such, the electrode significantly affects the process's performance. During this process, highly oxidizing hydroxyl radicals are generated near the anode surface by electrolyzing water at high anodic potential [136].

$$H_2O \rightarrow {}^{\bullet}OH + H^+ + e^- \quad (1)$$

The oxygen evolution reaction occurs at low anodic potential, and the generation of hydroxyl radicals occurs simultaneously. Choosing the right electrode material is crucial to produce hydroxyl radicals while avoiding side reactions such as oxygen evolution. The nature of electrode materials strongly affects both selectivity and efficiency. Table 1 shows that some active anodes (Class 1), such as RuO_2, IrO_2, Pt and Graphite, are good candidates for oxygen evolution reaction due to their low overpotential. Meanwhile, some anodes (Class 2) with high overpotential for water splitting have an inert behavior and favor the generation of hydroxyl radicals. Examples of such anodes are SnO_2, PbO_2,

Table 2
Experimental setups and corresponding degradation efficiencies of PFASs remediations through EAOP using boron doped diamond.

Anode	Cathode/ Reference Electrode	Distance (cm)	Conditions	Current Density (mA/ cm^2)	Time (min)	Kinetics	%removal	Ref.
Nb-BDD (35 cm^2)	Nb-BDD (35 cm^2)	2	1000 ml 2.9 ppm PFBS; 11 ppm PFHxS; 15 ppm PFOS; 0.1 M Na_2SO_4 300 r/min	2.3	2880	Pseudo-first-order kinetics	45 % PFBS; 91 %PFHxS; 98 %PFOS	[149]
Ultra nanocrystalline BDD (42 cm^2)	Tungsten (42 cm^2)	0.8	100 ppm PFOA; 5000 ppm Na_2SO_4; 293 K;	20	360	First order kinetics 0.09348 min^{-1} k_{PFOS}	>93 % PFOA	[142]
Si/BDD(5 cm × 5 cm)	Pt (5 cm × 5 cm) /Hg/Hg_2SO_4 (PAR)	0.3	0.4 mM PFOS; 10 mM NaClO4; 295 K	20	28	Pseudo-first-order kinetics 0.13 min^{-1} k_{PFOS}	>95 % PFOS	[87]
BDD (70 cm^2)	Stainless steel (70 cm^2)	0.5	2000 ml 293 K; 1.65 ppm PFASs	50	600	First order kinetics	99.7 % PFASs	[150]
Si/BDD (2.5 cm × 3.4 cm)	Ti(2.5 cm × 3.4 cm)/SCE	3	40 ml 0.114 mM PFBA; 0.114 mM PFHxA; 0.114 mM PFOA; 0.114 mM PFDeA; 1400 ppm NaClO4; 330 K	0.59	120	Pseudo-first-order kinetics 0.0332 min^{-1} k_{PFBA} 0.0335 min^{-1} k_{PFHxA} 0.0428 min^{-1} k_{PFOA} 0.0455 min^{-1} k_{PFDeA}	97.48 % PFOA	[105]
BDD (77.4 cm^2)	Pt deposited Ti (77.4 cm^2) /Ag/AgCl (BAS)	1	300 ml 8 mM PFOA; 10 mM $NaClO_4$	0.15	480	Pseudo-first-order kinetics 0.000517 min^{-1} k_{PFBA}	~60 % PFOA	[140]
Ti/BDD (5 cm × 5 cm)	Ti electrode	1.5	100 mL PFNA or PFDA; 0.25 mmol/L with 10 mmol/L NaClO4	10	180	pseudo-first-order kinetic 0.023 min^{-1} k_{PFNA} 0.012 min^{-1} k_{PFDA}	98.7 ± 0.4 % PFNA 96.0 ± 1.4 % PFDA	[151]
BDD-type UNCD on a niobium substrate (11 cm × 11 cm)	Ti/IrO_2-Ta_2O_5	0.4	100 ml 5 ppm PFOS	30 ~ 50	70	pseudo-first order PFOS oxidation	>99 %	[93]
Niobium coated BDD (35.05 cm^2)	Niobium coated BDD (321.57 cm^2)	2	10 ppm PFOA 1.5 g/L Na_2SO_4 5.2 ~ 22.5 V	11.85 ~ 21.4	60 ~ 240		Up to 99.5 %	[95]
3 cm^2 BDD	3 cm^2 BDD		100 ml 130 ppb PFOA 790 ppb PFHxA 2810 ppb PFBS 3210 ppb PFBA 15 mM Na_2SO_4 at pH 7	100	180	higher pseudo-first order rate constant 0.0009 min^{-1} PFBA 0.0129 min^{-1} PFHxA 0.072 min^{-1} PFOA		[148]
4600 cm^2 BDD	4600 cm^2 Stainless steel		12 L min^{-1} 150 L 2.2 ~ 2.8 ppb PFAS	231A	550		Mean 77 % for long-chain Mean 22 % for short-chain	[147]

Ti_4O_7 and BDD, making them ideal anode electrodes for PFAS degradation.

As illustrated in Fig. 2, due to the short lifetime of hydroxyl radicals, EAOP only occurs in the vicinity of the electrode surface. Thus, it is crucial for contaminants to transfer from the bulk solution to the electrode surface. In this type of electrode, three stages must be completed: (1) The pollutants must transfer from the bulk solution to the electrode surface. (2) The pollutants react with hydroxyl radicals. (3) The resulting end products must transfer from the electrode surface back to the bulk solution.

The mass transfer rate of pollutants is shown in Eq. (2) [137].

$$r_{PFASs} = k_m S(C_{bulk} - C_{electrode}) \quad (2)$$

where r_P is the mass transfer rate of pollutants, g/s, k_m is the mass coefficient (m/s), S is the electrode surface, C_{bulk} denotes the pollutants concentration in the bulk concentration (g/m^3) and $C_{electrode}$ denotes the PFASs concentration in the electrode (g/m^3). If there are mass transfer limitations of PFASs, the concentration of pollutants at the anode surface can be neglected. Thus, the rate of the process can be simplified to Eq. (3).

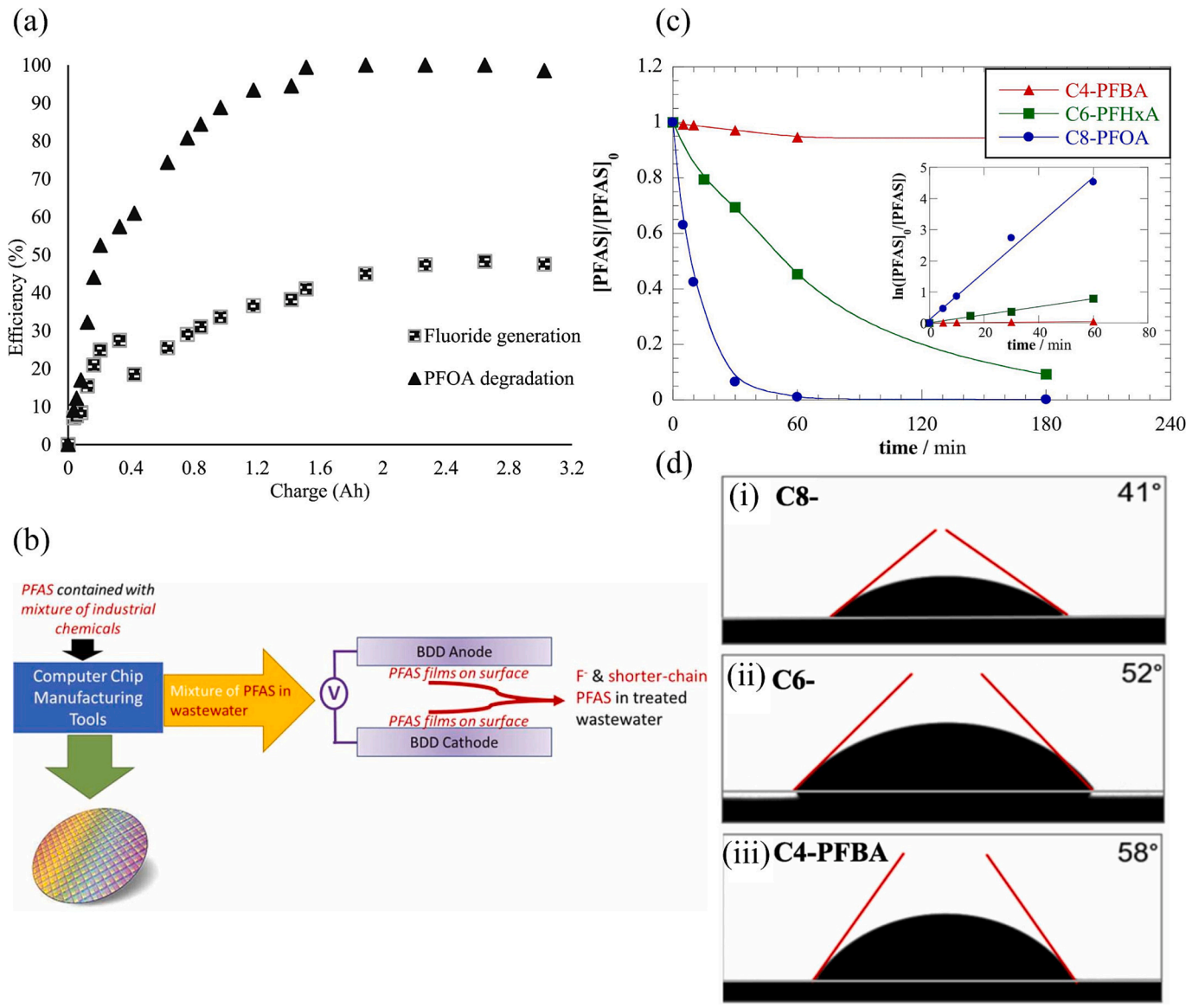

Fig. 4. (a) PFOA degradation and defluorination using BDD electrode [95]; (b) Setup of BDD electrodes for degradation of PFAS-contaminated wastewater; (c)PFOA degradation with BDD electrodes [148]; (d) Surface contact angle of PFOA, PFHxA and PFBA. and .
Reproduced with permission from [95][148]

$$r_p = k_m S C_{bulk} \tag{3}$$

If there are no mass transfer limitations, the rate of the electrochemical oxidation of pollutants could be written as

$$r_p = \frac{j^* S}{nF} \tag{4}$$

where j denotes the effective current density for contaminates destruction, S denotes electrode area, n is the charge number of the electrode reaction and F is the Faraday constant.

The electrochemical oxidation of contaminants in the bulk solution requires the electrochemical generation of a mediator, which can occur at either the anode or cathode electrode surface. These mediators then transfer to the bulk solution and react with PFASs. For example, the presence of SO_4^{2-} can generate $S_2O_8^{2-}$, the presence of Cl^- can produce Cl_2, $HClO$, $HClO_2$, $HClO_3$ and $HClO_4$. $Fe^{2+/3+}$ is a media that activates the Fenton reaction.

2.2. Electrochemical oxidation of PFASs

Due to the strong C–F band, synergistic effects of direct electron transfer and hydroxyl radicals decompose PFAS at high anodic overpotentials, where radicals with strong oxidizing and nonselective abilities are produced including •OH, O_2^-•, SO_4^-• and CO_3^-•. They could be divided into two groups depending on where the predominant reactions take place: the surface of the electrodes or the bulk solutions.

During the electrochemical oxidation of PFAS on the surface of the electrodes, the PFAS molecules are attracted to the anode surface and undergo degradation through an electron transfer reaction [138]. The hydroxyl radicals produced by electrochemistry only exist on the surface of the anode because they have a very short lifetime of only 2 ~ 4 μs. Therefore, the direct electrochemical oxidation of PFASs only occurs on the surface of the anode. In contrast, indirect oxidation occurs in the solution through the oxidants produced by cathodic reactions [138]. The remediation of PFASs by direct oxidation on the anode surface is suitable for concentrated and low-volume streams.

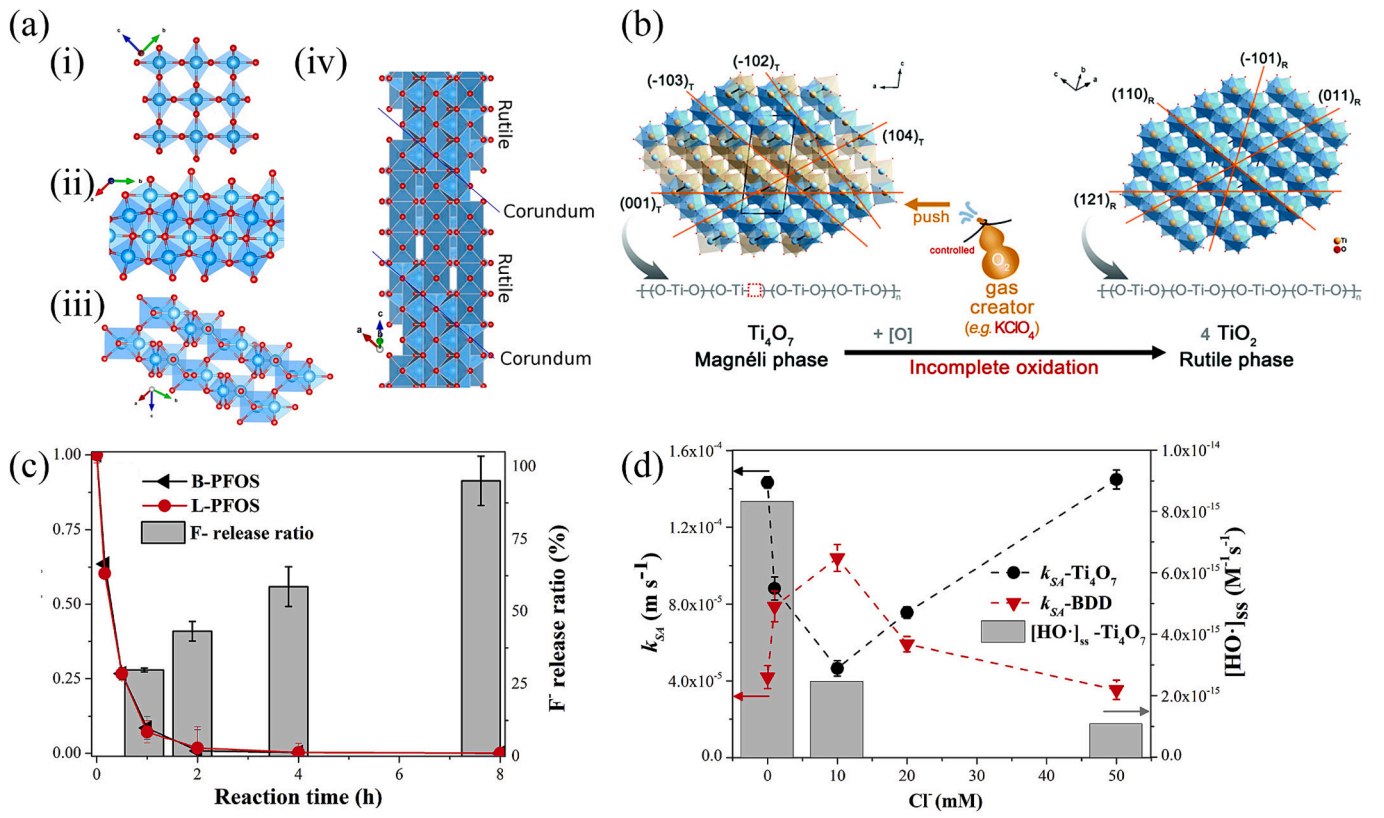

Fig. 5. (a) Different structure of titanium oxide, include (i) rutile (ii, iii) corundum, and (iv) Magnéli phase Ti_4O_7 structure [155]; (b) Schematic diagram of preparation of black Magnéli phase Ti_4O_7 [153]; (c) Degradation of PFOS and F^- release during electro-oxidation on Ti_4O_7 electrode; (d) The rate constant (k_{SA}) and the steady-state concentration of $HO^·$ for PFOS degradation during electrooxidation on Ti_4O_7 or BDD anode in the presence of Cl^- [134]. and Reproduced with permission from [155,153][134].

2.3. Configuration of electrochemical oxidation advanced oxidation process

The EAOP oxidation rates of contaminants are limited by either chemical or mass transport processes and are driven by the current flow. Thus, to maximize the system efficiency, it is important to minimize the resistance in chemical or mass transport processes, as well as minimize the ohmic resistance and use the main voltage to overcome the overpotential of the electrodes. Therefore, the configuration of the EAOP cell is important. As shown in Fig. 3a, it contains two electrodes with a distance of less than 1 cm in a batch electrode operation. The diffusion resistance in the chemical or mass transport processes can be minimized by stirring the solution. In addition, flow-through and flow-through designs ensure a continuous supply of reactants to the electrode surface and efficient removal of reaction products. Therefore, either a flow-through (Fig. 3b) or flow-through (Fig. 3c) setup can be used to minimize resistance.

3. Anode electrode materials

In recent years, various novel EAOP technologies have been studied and applied in wastewater treatment and remediation of industrial contaminants [139]. Pollutants remediation by EAOPs have shown promising results at the lab scale. However, the practical applications of these technologies are still rare. Novel electrode materials with higher electrochemical activity and material stability, along with optimization of reactor geometry and fluid dynamics have been introduced. Recently, the EAOPs technology has been upscaled to pilot plants, making progress towards commercialization [139].

The choice of anode materials of EAOPs is critical for efficient pollutant remediation. Anode materials are typically categorized as: (i) metal-oxide, including Tin-, lead- and Titanium based materials, and (ii) non-metal oxide, including boron-doped diamond (BDD) material (shown in Table 2). Tin and lead based electrodes have been found to be less effective and may pose issues due to the leaching of toxic metals, while the BDD electrode has shown high efficiency and stability in degrading PFASs [85,88,105,140–142]. The BDD electrodes are made of boron-doped microcrystalline diamond with a relatively large grain size ranging from 0.5 to 10 μm, resulting in pinholes and defects [143]. The problem is overcome by using ultra-nanocrystalline boron-doped diamond with small grain sizes of 2–5 μm, which provides better performance than standard BDD material [6]. Silicon is the most compatible substrate for BDD electrodes due to its ability to form a self-limiting oxide and its inert electrochemical activity. However, the silicon substrate is very brittle, which limits its use in many applications [143]. Despite these challenges, the development of novel electrode materials with higher electrochemical activity and stability remains a crucial area of research to further enhance the performance of EAOPs in practical applications.

3.1. Boron-doped diamond electrode

Pure diamond is not suitable for electrode material due to its extremely high inherent electrical resistivity. However, after doped with boron, Boron-doped diamond (BDD) contains an inert electrochemical activity matrix consisting of crystalline (sp^3) (diamond) and amorphous (sp^2) (non-diamond) carbon phases [144]. As a result, BDD becomes conductive and corrosion-resistant with the increasing boron doping level. This property has made BDD an excellent electrode material with superior material characteristics.

Due to the large amount of non-active matrix of crystalline (sp^3), the BDD electrode is electrocatalytically inert. It has the largest

Table 3
Experimental setups and corresponding degradation efficiencies of PFASs remediations through EAOP using metal-oxide anodes.

Metal-Oxide									
Anode	Cathode/ Reference Electrode	Distance (cm)	Conditions	Current Density (mA/cm^2)	Time (min)	Chemicals	Kinetics	%removal	Reference
Magneli phase Ti_4O_7(Ti_4O_7) (10 cm × 5 cm)	Stainless Steel Sheet (10 cm × 5 cm)/SCE	1.5	200 ml, 0.5 mM PFOA, 0.1 mM PFOS, 20 mM NaClO4,	5	180	98 % PFOA; 98 % PFOS	Pseudo-first-order kinetics, 0.034 min^{-1} k_{PFOA} 0.013 min^{-1} k_{PFOS}	99.9 % PFOA, 93.4 % ± 3.4 PFOS	[157]
Magneli phase Ti_4O_7(Ti_4O_7) (10 cm × 5 cm)	Stainless Steel Sheet (10 cm × 5 cm)/NA	2.5	100 ml 10 ppm PFOS; 10 ppm PFOA; 100 mM Na_2SO_4	10	180	High purity PFOA and PFOS (Sigma Aldrich Co.)	Pseudo-first-order kinetics 0.0491 min^{-1} k_{PFOS} 0.0226 min^{-1} k_{PFOA}	98.9 % PFOS 96 % PFOA	[158]
Titanium mesh coated with Magnéli-phase titanium suboxides Ti_nO_{2n-1} (11 cm × 11 cm)	Ti/IrO_2-Ta_2O_5 (11 cm × 11 cm)	0.4	100 ml 5 ppm PFOS	30 ~ 50	70	98 % PFOS	pseudo-first order PFOS oxidation	>99 %	[93]
Ti/SnO_2-Sb/Ce-PbO_2 (Ce-PbO_2) (10 cm × 5 cm)	Stainless Steel Sheet (10 cm × 5 cm)/SCE	1.5	200 ml, 0.5 mM PFOA, 0.1 mM PFOS, 20 mM NaClO4,	5	180	98 % PFOA; 98 % PFOS	Pseudo-first-order kinetics, 0.02 min^{-1} k_{PFOA} N/A k_{PFOS}	99.5 % ± 0.9PFOA, N/A PFOS	[157]
Ti/SnO_2-Sb (12 cm × 5 cm)	Ti (12 cm × 5 cm)/SCE	1	100 ml 100 ppm PFOA, 10 mmol/L NaClO4, pH = 5	10	90	98 %PFOA	Pseudo-first-order kinetics	#####	[88]
Ti/SnO_2-Sb/PbO_2 (12 cm × 5 cm)	Ti (12 cm × 5 cm)/SCE	1	100 ppm PFOA, 10 mmol/L NaClO4, pH = 5	10	90	98 %PFOA	Pseudo-first-order kinetics	#####	[88]
Ti/SnO_2-Sb/MnO_2 (12 cm × 5 cm)	Ti (12 cm × 5 cm)/SCE	1	100 ppm PFOA, 10 mmol/L NaClO4, pH = 5	10	90	98 %PFOA	Pseudo-first-order kinetics	#####	[88]
Ti/BDD (BDD) (10 cm × 5 cm)	Stainless Steel Sheet (10 cm*5cm)/SCE	1.5	200 ml 0.5 mM PFOA, 0.1 mM PFOS, 20 mM NaClO4	5	180	98 % PFOA; 98 % PFOS	Pseudo-first-order kinetics 0.027 min^{-1} k_{PFOA} N/A k_{PFOS}	98.8 % ± 1.9 PFOA NA PFOS	[157]
Ti/SnO2-Sb2O5/PbO2-1.0 wt%PVDF (42 mm × 42 mm)	Ti (42 mm × 42 mm)/NA	1	200 ml 100 ppm PFOA; 1400 ppm NaClO4; 1300r/min; pH = 3	40	180	95 % PFOA (Sigma-Aldrich Co.)	Pseudo-first-order kinetics 0.01384 min^{-1} k_{PFOA}	92.1 % PFOA	[85]
Ti/SnO2-Sb/Yb-PbO2 (5 cm × 2 cm)	Ti(5 cm × 2 cm)/NA	0.5	200 ml 100 ppm PFOA; 0.1 M Na_2SO_4; 298 K; pH = 5	20	150	95 % PFOA (Wong jiang)	Pseudo-first-order kinetics 0.0193 min^{-1} k_{PFOA}	95.11 % ± 3.9 %	[159]
Ti/SnO2-Sb-PbO2(5 cm × 2 cm)	Ti(5 cm × 2 cm)/NA	0.5	200 ml 100 ppm PFOA; 0.1 M Na_2SO_4; 298 K; pH = 5	20	150	95 % PFOA (Wong jiang)	Pseudo-first-order kinetics 0.012 min^{-1} k_{PFOA}	83.94 % ± 1.6 %	[159]
Ti/SnO2-Sb-Yb(5 cm × 2 cm)	Ti(5 cm × 2 cm)/NA	0.5	200 ml 100 ppm PFOA; 0.1 M Na_2SO_4; 298 K; pH = 5	20	150	95 % PFOA (Wong jiang)	Pseudo-first-order kinetics 0.011 min^{-1} k_{PFOA}	80.14 % ± 3.8 %	[159]

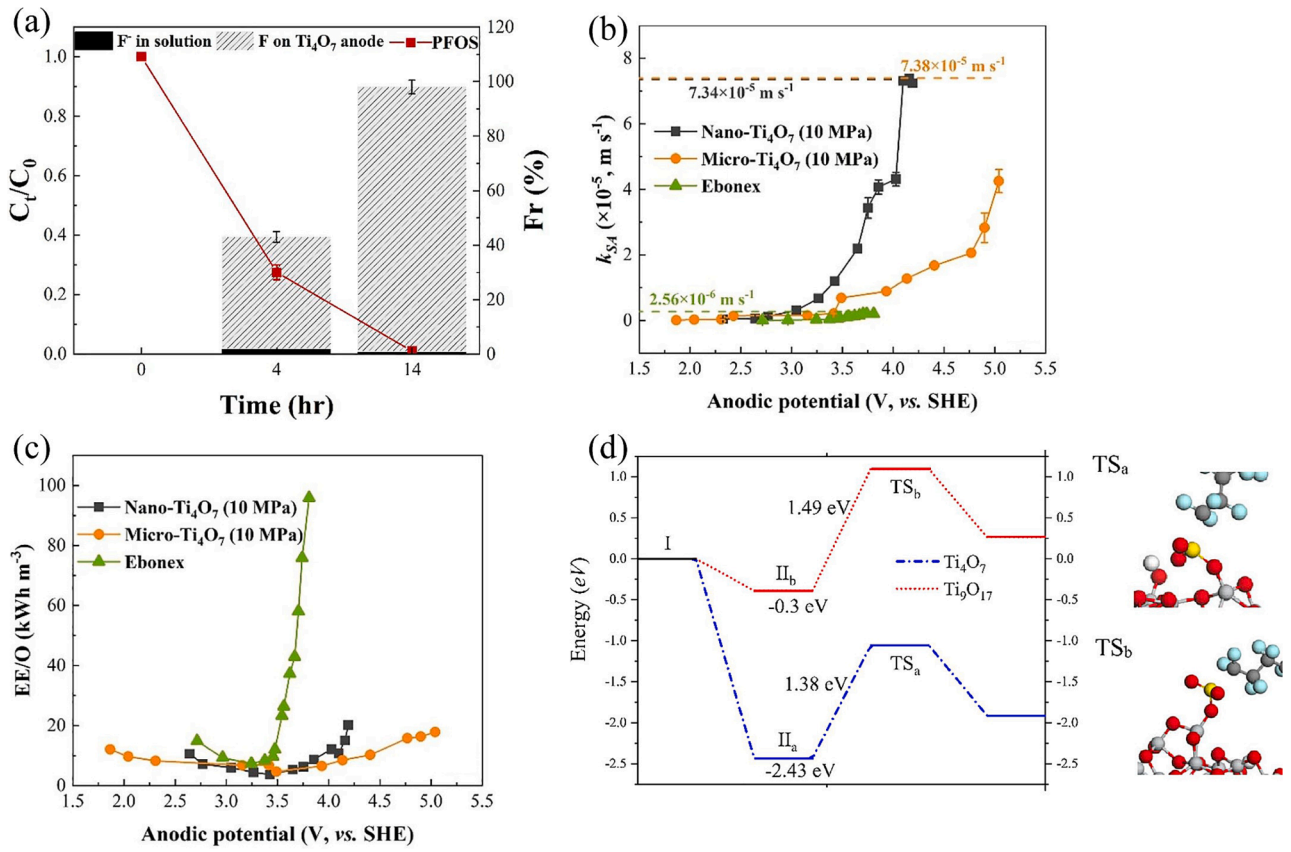

Fig. 6. (a) PFOS removal and defluorination ratio with time; (b) PFOS degradation rate constant in relation to the anodic potential (vs. SHE) with Ebonex, nano-Ti_4O_7 and micro-Ti_4O_7 anode; (c) Energy consumption in relation to the anodic potential for PFOS degradation; (d) The energetics of PFOS interaction with Ti_4O_7 and Ti_9O_{17} [154]. .
Reproduced with permission from [154]

electrochemical potential solvent window (3.7 V) and poor oxygen reduction reaction (ORR) activity compared to glassy carbon (GC), which is more catalytically active due to a significant amount of sp^2 carbon with a smaller solvent window (1.0 V) [145,146]. These properties enable BDD anodes to promote the generation of hydroxyl radicals, which unselectively degrade organic pollutants with a high current efficiency:

$$BDD + H_2O \rightarrow BDD(\cdot OH) + H^+ + e^- \quad (5)$$

$$BDD(\cdot OH) + R \rightarrow BDD + CO_2 + H_2O \quad (6)$$

Table 2 summarizes the experimental setups and the corresponding PFASs degradation efficiencies through EAOP using boron-doped diamond as the anode. Different dopes, including Nb, Si, Ti and nano BDD, were used. Anode sizes vary from 8.5 cm^2 [105] in laboratory size to 4600 cm^2 in pilot scale [147]. The highest removal efficiency reached up to 99.7 % with pure BDD. Jean et al. [95] investigated Niobium coated BDD as both the anode and cathode for EAOP of 10 ppm PFOA. They achieved up to 99.5 % destruction of PFOA while the defluorination was only up to 50 %, indicating the formation of some short-chain PFAS during the process, (e.g. PFBA, PFPeA, PFHxA) (Fig. 4a). Recently, Nienhauser [148] employed BDD plates as both the anode and cathode electrodes to treat PFAS-contaminated industrial wastewaters (Fig. 4b). The significant difference in the rate of PFAS degradation may be attributed to the interaction between PFAS and the electrode surface (Fig. 4c), which is also confirmed by surface contact angle experiments (Fig. 4d). These findings validate the hypothesis that an increase in the length of the surfactant chain promotes the interaction between PFAS and the electrode, leading to better removal of longer PFAS chains.

Recently, Smith et al. [147] conducted a pilot study demonstrating a practical treatment approach for PFAS in groundwater and landfill leachate. Their method combines foam fractionation to concentrate PFAS, followed by electrochemical oxidation (EO) to degrade them. They used a 20-liter flow cell with 23 boron-doped diamond (BDD) plates (5 × 20 cm) as anodes and 24 stainless steel plates (5 × 20 cm) as cathodes, with a 3 mm spacing between them. The total active area of each electrode was 4600 cm^2. A constant current of 231A was applied on this cell for 540 min. The average total PFAS degradation achieved by the designed treatment process was 50 %. Long-chain PFAS were degraded by up to 86 %, while short-chain PFAS saw a degradation of up to 31 %. They found that energy consumption depends mainly on the amount of treatment. After 540 min of treatment, the energy consumption of the 50-liter experiment was about 270 kWh/m^3, while the energy consumption of the 150-liter experiment was about 93 kWh/m^3, about one-third.

3.2. *Magnéli-phase Ti_4O_7 electrode*

Titanium dioxide (TiO_2) is a common semiconductor photocatalyst. Interestingly, the electronic conductivity of TiO_2 can be completely altered by adjusting its oxygen deficiencies to Magnéli phase titanium sub-oxides, Ti_nO_{2n-1} ($3 < n < 10$). Its electrical conductivity varies from tens to several thousand S cm^{-1} depending on its oxygen deficiencies [152]. Magnéli-phase titanium oxides are usually a mixture of stoichiometries. These materials have a unique crystal structure with each layer containing a different ratio of titanium to oxygen leading to the creation of shear planes where 2D chains of octahedra become face-sharing to compensate for local deficiencies of oxygen (Fig. 5a). This unique structure results in a high electrical conductivity similar to that of metals and a great corrosion resistance close to that of ceramic

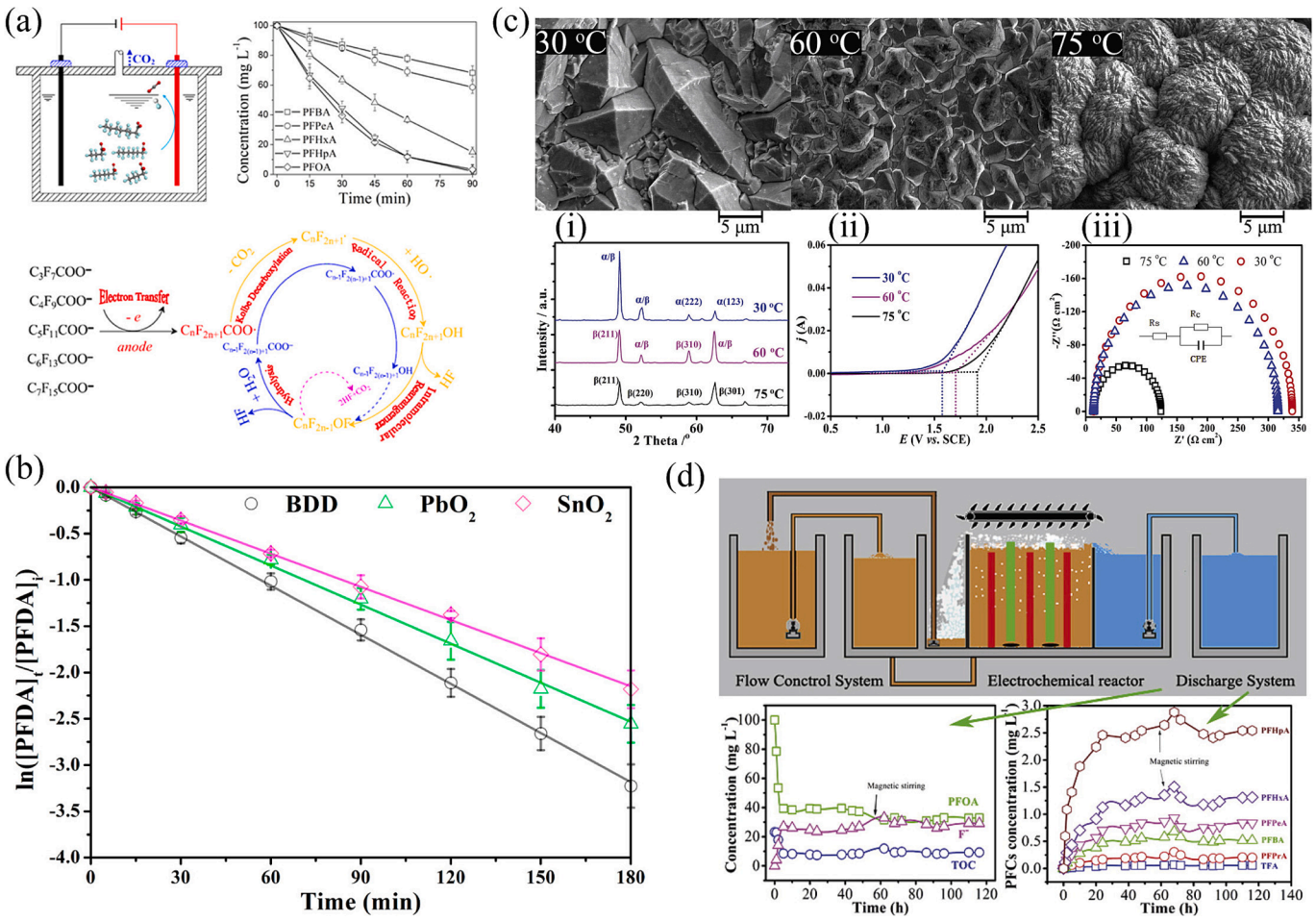

Fig. 7. (a)Proposed mechanism of the electrochemical degradation of PFAS [165]; (b) Logarithmic PFDA concentration on BDD, PbO_2 and SnO_2 electrodes as a function of electrolysis time [151]; (c) Surface morphology and electrochemical characterization of Zr-PbO_2 doped at different bath temperatures. (i) X-ray diffraction; (ii) V-I curves; (iii) Impedance spectra; (d) Illustration of the continuous setup for PFOA treatment (up) and the concentrations of PFOA, F-, TOC and PFCs changed with the reaction time During the electrolytic treatment of PFOA (down)[166]. and .
Reproduced with permission from [151][166]

materials. For example, the electrical conductivity of Ti_4O_7 is ~1000 S/cm. The projected half-life of Ebonex® is 50 years in 4 mol/L H_2SO_4 at room temperature [152]. Additionally, Ti_4O_7 also has a higher overpotential for oxygen evolution potential (+2.6 V vs standard hydrogen electrode, SHE) than BDD. These properties make Ti_4O_7 a suitable candidate for wastewater treatment, cathodic protection, bipolar battery, as well as water splitting. Based on the thermodynamics analysis, the reduction of well-crystallized TiO_2 does require harsh reaction conditions. Fig. 5b shows a typical method to prepare black Magnéli phase Ti_4O_7 [153]. A mixture of Ti_4O_7 and $KClO_4$ was heated at 600 °C for 2 h and the amount of oxygen was controlled by the decomposition of $KClO_4$. Thus, an appropriate amount of oxygen in Ti_4O_7 is controlled. The other method is high temperature sintering followed by hydrogen reduction at high temperature [134,154].

Table 3 shows the experimental setups and corresponding degradation efficiencies of PFASs remediations by EAOP using metal-oxide anodes. Titanium suboxide (Ti_4O_7) has been reported as an effective and cost-efficient electrode material in PFAS treatment due to its potentially low cost in commercial production, good conductivity, high stability and robustness [156]. Promising results have been obtained in early research on the remediation of PFOA and PFOS using the titanium-based electrodes with a potential by-product formation of less than 1 % [157]. However, further studies are required for the commercial application of this novel material in the degradation of PFASs, and the formation of by-products needs to be further assessed. Liang et al. [158] investigated EPOA of PFOA and PFOS with a Magnéli phase Ti_4O_7 electrode. After 3 hr of electrolysis in a 100 ml of 100 mM Na_2SO_4 solution containing 10 ppm of PFOA or PFOS, the removal efficiency of PFOA and PFOS was 96 % and 98.9 %, respectively. Furthermore, the EAOP was also applied to the removal of high concentrations of PFOA (100.5 ppm) and PFOS (68.6 ppm) [158]. The electrolysis process resulted in the removal of up to 77.2 % of PFOA and 96.5 % of PFOS after 17 h. They also claimed that the concentration of PFOA and PFOS was below the limits of quantification after treatment. Wang et al. [134] investigated the degradation of (PFOS) in an electrochemical system using Magnéli phase Ti_4O_7 electrode as the anode (Fig. 5c). The effect of chlorides on the treatment process was examined and compared to that of a boron-doped diamond (BDD) electrode (Fig. 5d). The degradation of PFOS was found to occur through a combination of direct electron transfer (DET) and attack by anodic surface-absorbed hydroxyl radicals formed by anodic oxidation of water. The presence of Cl^- inhibited the degradation of PFOS on the Ti_4O_7 electrode by inhibiting the oxidation of water but accelerated the degradation of PFOS on the BDD electrode, where the oxidation of Cl^- by DET occurred. The advantage of the Ti_4O_7 electrode is that the formation of chloride and perchlorate is slower on Ti_4O_7 than on the BDD anode. Later, Wang et al. [154] investigated the effect of different porous structures on the degradation of PFOS. The electrooxidation of PFOS was evaluated in batch and REM systems using three different anodes, including commercial Ebonex, nano-Ti_4O_7 and micro-Ti_4O_7. As shown in Fig. 6a, almost complete defluorination was achieved. In both

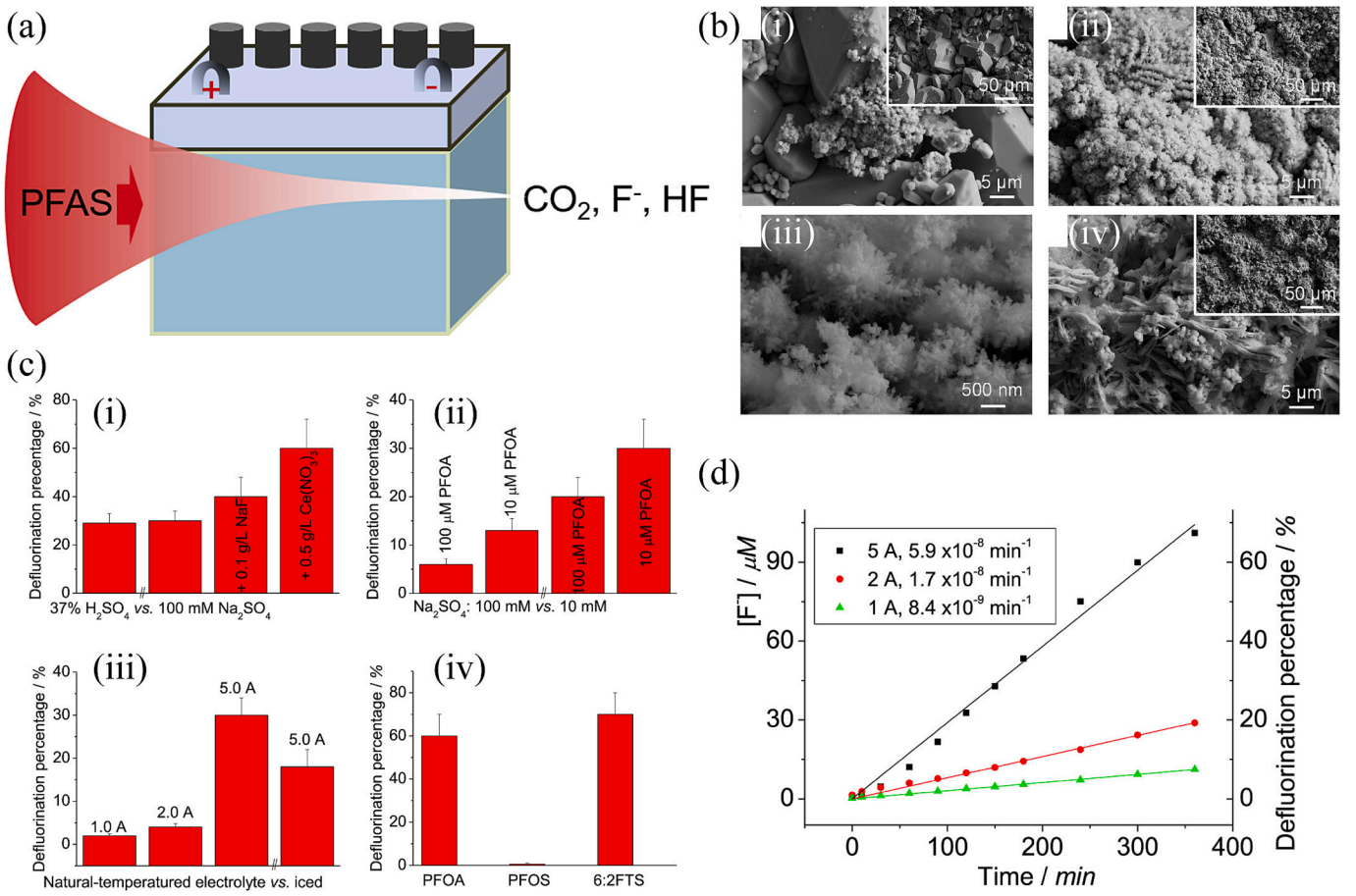

Fig. 8. (a) Schematic of the experiment setup; (b) SEM characterization of electrodes before (a) and (b-c) after the activation, (d) the surface of the cathode; (c) Effect of the activation electrolyte (i), the PFAS concentration (ii), current (iii) and PFAS species (iv) on the defluorination; (4) F^- concentration with different current with time [167]. .
Reproduced with permission from [167]

batch and REM operations, the nano-Ti_4O_7 anode outperformed the micro-Ti_4O_7 anode in terms of PFOS degradation rate and energy efficiency, mainly due to its favorable pore size distribution (Fig. 6b). The performance of PFOS degradation largely depends on the composition of the anode. Compared with the Ebonex (Ti_9O_{17}) anode, the Ti_4O_7 anode exhibited higher PFOS degradation rate and energy efficiency (Fig. 6c). DFT calculations revealed that a larger proportion of Ti^{3+} ions in Ti_4O_7 facilitates the uptake of PFOS and lowers its activation barrier for direct electron transfer in Fig. 6d.

3.3. Lead dioxide electrode

Lead dioxide is one of the n-type metal oxides which show high electron mobilities. The conductivity of α-PbO_2 is close to 103 Ω^{-1} cm^{-1} while one of the rutile (β-PbO_2) is close to 104 Ω^{-1} cm^{-1} [160]. Lead dioxide has drawn tremendous attention as a potential electrode due to its widespread use as the positive plate in lead-acid batteries. Metal oxides are normally non-conductors or semiconductors while some metal oxides have high electrical conductivity close to metals. Lead dioxide is one of them, and has an electrical double layer formed in the interphase between the lead dioxide electrode and an electrolyte solution. Lead dioxide is polymorphic, including orthorhombic α-PbO_2 and tetragonal β-PbO_2 [161]. A mechanism of high electrical conductivity is proposed, that is, lead dioxide is not a precise stoichiometric composition, but contains an excess of lead, which is decomposed into tetravalent lead ions and free electrons. The latter leads to such a high electrical conductivity [162]. All lead (iv) ions are localized in the centre of a distorted octahedron and the essential difference between them lies in the pacing method. The adjacent octahedra of α-PbO_2 share non-opposite edge so that zig-zag chains are formed. Through shared corners, each chain is also connected to the next one. For tetragonal Rutile (β-PbO_2), neighbouring octahedra share opposite edges, resulting in the formation of linear chains of octahedra. Each chain is connected with the next one through shared corners [163,164].

Niu et al. [165] electrodeposited the Ce-doped PbO_2 film electrode for electrochemical oxidation of PFAS, including PFBA, PFPeA, PFHxA, PFHpA, and PFOA in an aqueous solution (100 mL of 100 mg/L). The electrochemical oxidation of PFAS follows the pseudo-first order kinetics and after 90 min of electrolysis, the removals of these PFAS species are 31.8 % ± 4.6, 41.4 % ± 4.1, 78.2 % ± 3.2, 97.9 % ± 4.6, and 96.7 % ± 3.0, respectively. The primary end product of this process is F^- as well as small amounts of intermediates in an aqueous solution. They also proposed a possible pathway of the electrochemical oxidation of PFAS (See Fig. 7a).

Lin et al. [151] prepared Ti/Ce–PbO_2 (PbO_2) electrodes by electrodeposition and investigated the electrochemical oxidation of PFAS, including 0.25 mmol/L of perfluorononanoic acid(PFNA) and 0.25 mmol/L of perfluorodecanoic acid (PFDA) at room temperature. After 180 min electrolysis, the removals of PFNA and PFDA are 97.1 % and 92.2 %, respectively. In the aqueous solution after electrolysis, the main end product of this process is F^-, as well as some trace amounts of intermediates. For the secondary contamination, the part of the electrode (Pb) was dissolved and the content of Pb ions was detected to be only 0.004 and 0.005 mg/L for PFDA and PFNA solutions, respectively. The

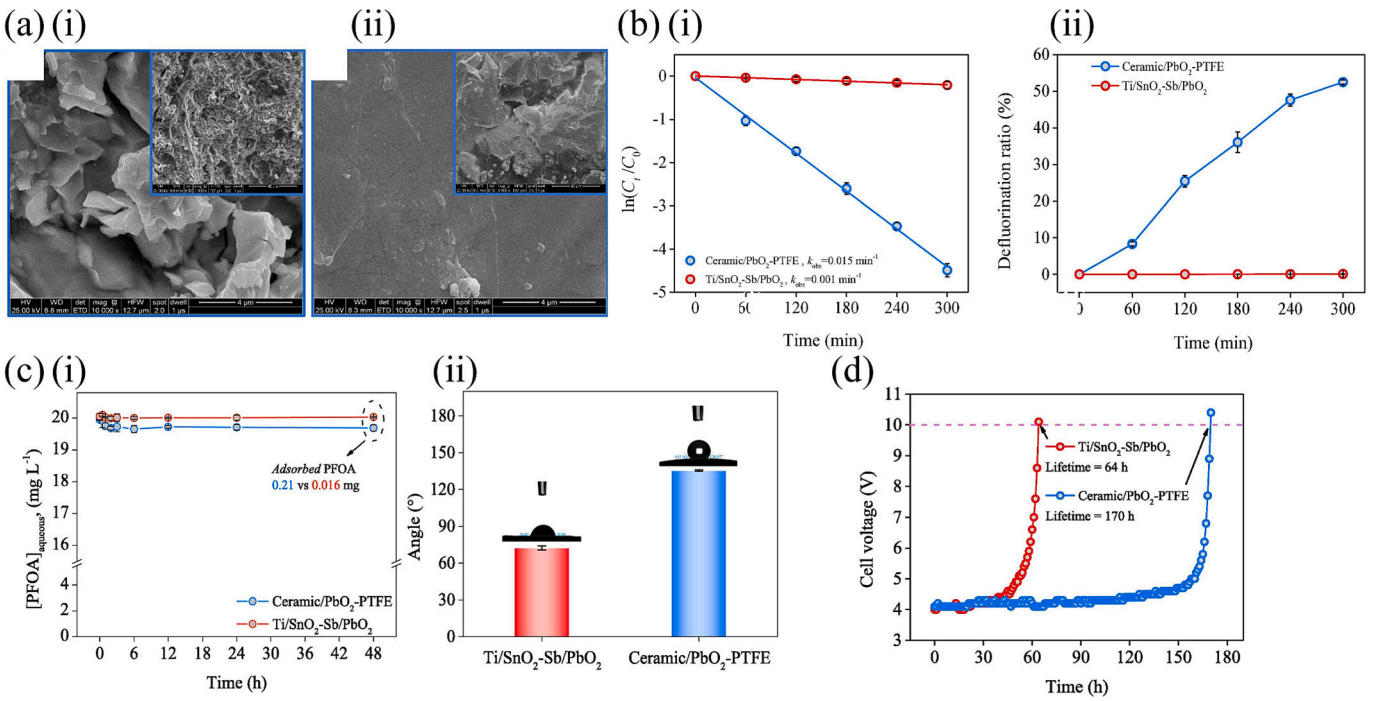

Fig. 9. (a) Morphology of (i) Ti/SnO_2-Sb/PbO_2 and (ii) ceramic/PbO_2-PTFE anodes; (b)(i) Pseudo-first-order kinetic diagram with two anodes, (ii). The defluorination rate of PFOA by two anodes; (c)(i) PFOA adsorbed on the anode after 48 h equilibration; (ii) Water contact angle on the anode; (d) Stability performance of two anodes for PFOA destruction [168]. .
Reproduced with permission from [168]

concentrations of lead ions are lower than the drinking water regulations (0.01 mg/L) of the U.S. Environmental Protection Agency (USEPA). No Ce ions were detected in all samples. Therefore, it is safe to employ the PbO_2 anode for wastewater treatment based on their results. They also propose three potential routes as a degradation mechanism, including (1) Removal of CF_2 to form short-chain PFAS; (2) Direct oxidation to HF and CO_2; (3) Formation of volatile fluorinated organic compounds. Their results demonstrated that the electrochemical oxidation method with PbO_2 as electrode could be a high efficiency in oxidising PFNA and PFDA for wastewater treatment. They also prepared Ti/SnO_2–Sb–Ce (SnO_2), Ti/SnO_2–Sb/Ce–PbO_2 (PbO_2), and Ti/BDD (BDD) anodes under galvanostatic control at room temperature for PFDA treatment. As shown in Fig. 7b, they compared the PFDA destruction performance on three electrodes, indicating an apparent pseudo-first-order reaction (diffusion-controlled). At 180 min, the removal rate of PFDA by the SnO_2, PbO_2 and BDD electrode is 88.7 %, 92.2 % and 96.0 %, respectively. It is obvious that the BDD shows the best performance.

Xu et al. [166] prepared Zr-doped nanocrystalline PbO_2 (Zr-PbO_2) film electrodes at different bath temperatures (Fig. 7c). A continuous setup for PFOA treatment was established (Fig. 7d) to study the long-term stability performance of PFOA wastewater treated by 75-Zr-PbO_2 (doped at 75 °C) electrolysis. The concentrations of PFOA, TOC, and F^- in the outlet water of the discharge system were monitored. After electrolysis for 5 h, the concentration of PFOA decreased rapidly, and the removal efficiency of PFOA reached more than 60 %. The F- concentration increased from 0 ppm to 26.8 ppm while the TOC concentration also decreased significantly.

Cheng et al. [167] employed lead peroxide (PbO_2) plates from car battery as an electrode from a lead-acid battery to decompose PFOA, 6:2 FTS, and PFOS. Fig. 8a shows the schematic of the experimental setup while Fig. 8b presents the morphology of the anode electrode surface before and after activation as well as the cathode surface morphology. They also investigated the effect of the different activation electrolyte, PFAS removal electrolyte, current and PFAS species on the defluorination of PFAS (Fig. 8c and d). After optimisation, they successfully removed >99 % PFAS whilst mineralising ~59 % PFOA. The high PFAS removal is arising from the strong adsorption and oxidation due to the high specific surface area. However, leaching of HF and Pb^{2+} may lead to secondary contaminants.

Lou et al. [168] recently fabricated Ti/SnO_2-Sb/PbO_2 and ceramic/PbO_2-PTFE anodes for efficient ppm-level PFOA destruction (Fig. 9a and b). Doping PTFE into the PbO_2 coating increases its adhesion to electrodes and reduces its surface tension. Thus, doping PTFE into the PbO_2 coating not only increases the PFOA destruction rate but also boosts the defluorination ratio of PFOA. Later, they found that not only the ceramic/PbO_2-PTFE surface has a strong affinity for PFOA but also Ceramic/PbO_2-PTFE with PTFE dopant has a hydrophobic surface with a large water contact angle (135.4°), while the Ti/SnO_2-Sb/PbO_2 surface is hydrophilic (72.3°) (Fig. 9c). The stability performance of the ceramic/PbO_2-PTFE anode shows the better performance than the Ti/SnO_2-Sb/PbO_2 anode (Fig. 9d).

3.4. Tin dioxide electrode

Pure SnO_2 belongs to an *n*-type semiconductor with low conductivity and a band gap of 3.5 eV at room temperature; therefore, it is not directly suitable for an electrode material. But doping with other elements (such as Sb, Bi, F etc.) can improve the electrical conductivity [133]. Antimony-doped SnO_2 electrode has a high conductivity and a high overpotential for oxygen evolution of about 1.9 V relative to SHE (600 mV higher than Pt), which makes it suitable for anodizing organic pollutants including PFOA as attractive electrode materials.

Zhuo et al. [169] used a Ti/SnO_2-Sb-Bi electrode to investigate the electrochemical oxidation of PFOA (Fig. 10a and b). Over 99 % of 50 mg/L PFOA solution was decomposed with the first-order kinetic constant of 1.93 h^{-1} after 2 h of electrolysis (Fig. 10c). Intermediate products were detected in the aqueous solution, such as short-chain perfluorocarboxyl anions including $C_6F_{13}COO^-$, $C_5F_{11}COO^-$, $C_4F_9COO^-$, $C_3F_7COO^-$, $C_2F_5COO^-$, and CF3COO$^-$. The concentration of

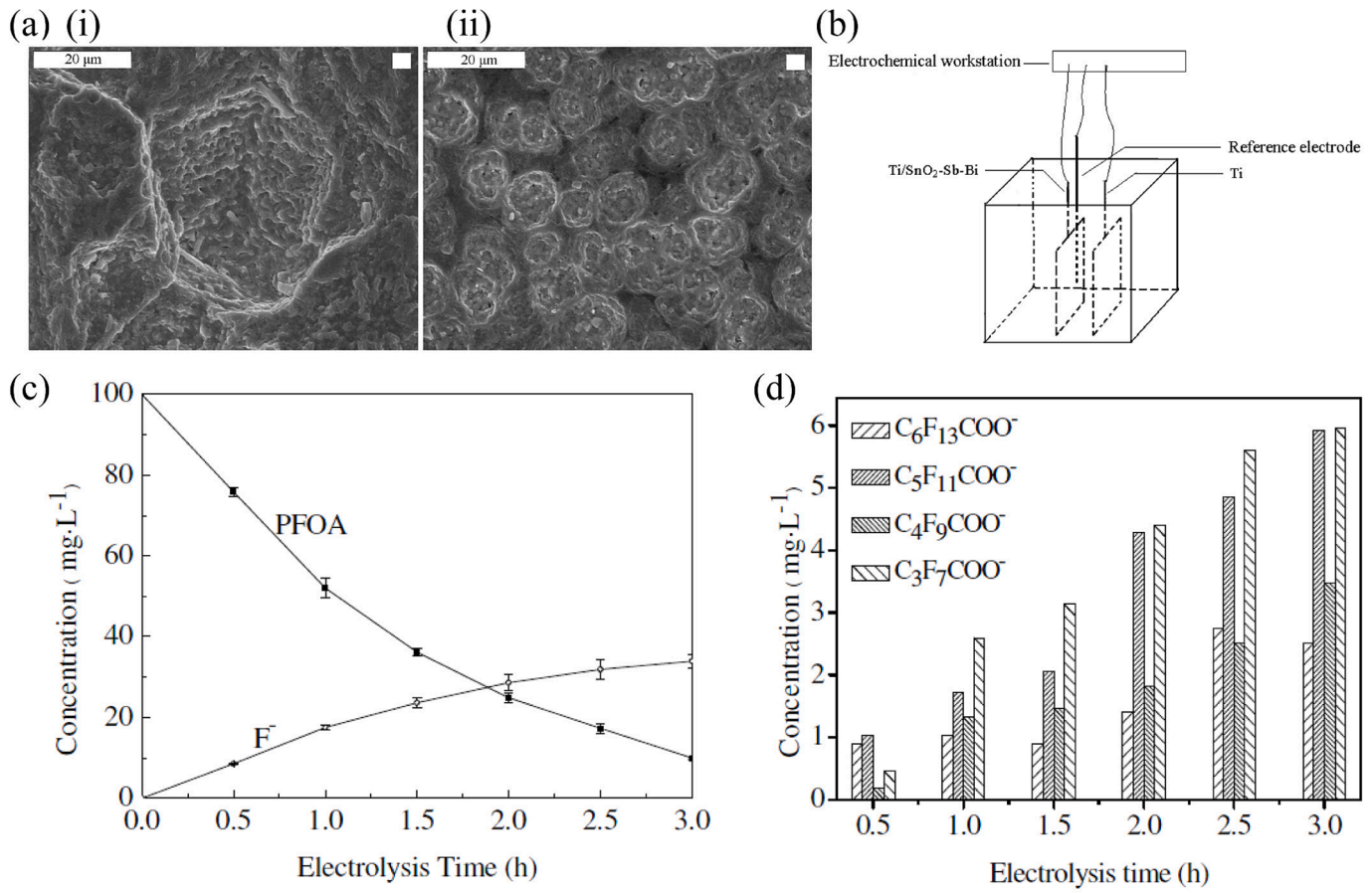

Fig. 10. (a) Morphology of Ti/SnO_2-Sb (left) and Ti/SnO_2-Sb-Bi electrode (right); (b) Setup of EAOP of PFOA in this study; (c) The changes of concentration of PFOA and F^- with time; (d) The changes of intermediates with time [169]. .
Reproduced with permission from [169]

intermediates increases with time (Fig. 10d). They also proposed an electrochemical oxidation mechanism of the PFOA decomposition. At a potential of 3.37 V (relative to the saturated calomel electrode, SCE), the carboxyl group of PFOA firstly transfers to the anode. Thereafter, the perfluoroheptyl radical is produced by the decarboxylation of the PFOA radical and it could react with hydroxyl radicals. It was found that the oxidation of PFOA on the Ti/SnO_2-Sb-Bi electrode starts from the carboxyl group in PFOA rather than C-C cleavage, followed by the CF_2 unzipping cycle. Lin et al. [151] prepared Ti/SnO_2–Sb–Ce electrode using a sol–gel technique and investigated the electrochemical oxidation of PFAS, i.e., 0.25 mmol/L of PFNA and PFDA solutions at room temperature. This SnO_2 electrode yielded a removal of 95.8 % PFNA and a removal of 88.7 % PFDA, the secondary pollution of Sb ions was spotted. In the aqueous solution, the primary end product is F^-, as well as some trace amounts of intermediates, after electrolysis.

3.5. Other anode materials

Recently, Nick and Jelena [94] developed a graphene sponge electrode (Fig. 11a) for electrochemically defluorination of C4-C8 PFAS. They found that the removal of the target PFAS increased with the anode current, while the performance deteriorated significantly at higher flow rates indicating that the electrochemical removal of PFAS was limited by mass transfer. The electrochemical degradation of long- and short-chain PFAS (PFOS, PFHxS and PFBS) was achieved through 74 %-87 % recovery of fluoride (Fig. 11d) at the highest applied current density (i.e. 23 mA cm^{-2}) with only estimated energy consumption of 9.4 ~ 10.8 kWh m^{-3}. For different PFAS, the percentages of electrosorption and electrooxidation decreased in the order of PFOS > PFOA > PFHxS > PFBA, and the defluorination and desulfonation present the similar trend as shown in Fig. 11b and c.

Jae-Hoon et al. [92] developed a nanoparticles (NPs)-embedded hydrogel nanofiber electrodes for PFAS destruction, include Ag NPs loaded poly acrylic acid (PAA)/(poly allylamine hydrochloride (PAH)-(carbon cloth) CC, Au NPs loaded PAA/PAH-CC, and Ag/Au NPs loaded PAA/PAH-CC (Fig. 12a). These nano metal particles led to a better electron transfer, and Ag/Au-PAA/PAH electrodes showed the lowest resistance and highest PFOA and PFOS oxidation rate. In Fig. 12b(i) and b(ii), compared with Ag-CNM, the Ag-coated hydrogel electrode (Ag-PAA/PAH) showed higher removal efficiency of PFOA and PFOS. Therefore, the PAA/PAH electrode was selected to be further investigated for electrochemical removal of PFAS. The electrochemical removal of PFOA and PFOS by Ag, Au and Ag/Au coated PAA/PAH coated electrodes were studied (Fig. 12b(iii) and b(iv)). Its energy consumption was estimated to be only 90 kWh m^{-3} for 91 % PFOS removal, and 164.9 kWh m^{-3} for 72 % PFOA removal, the initial concentration was only 1 ppb (Fig. 12c).

4. Electrolyte materials

Aqueous electrolytes are important components of Electrochemical Advanced Oxidation Processes. They could be wastewater, or usually a solution of a salt or salt mixture that provides the appropriate environment for ion conduction and promotes the production of oxidants.

Aqueous electrolytes make EAOPs more attractive for industrial-scale wastewater treatment because they have many advantages, including low cost, high stability, and inherent safety. To achieve the desired conductivity, sodium sulfate or sodium chloride is usually

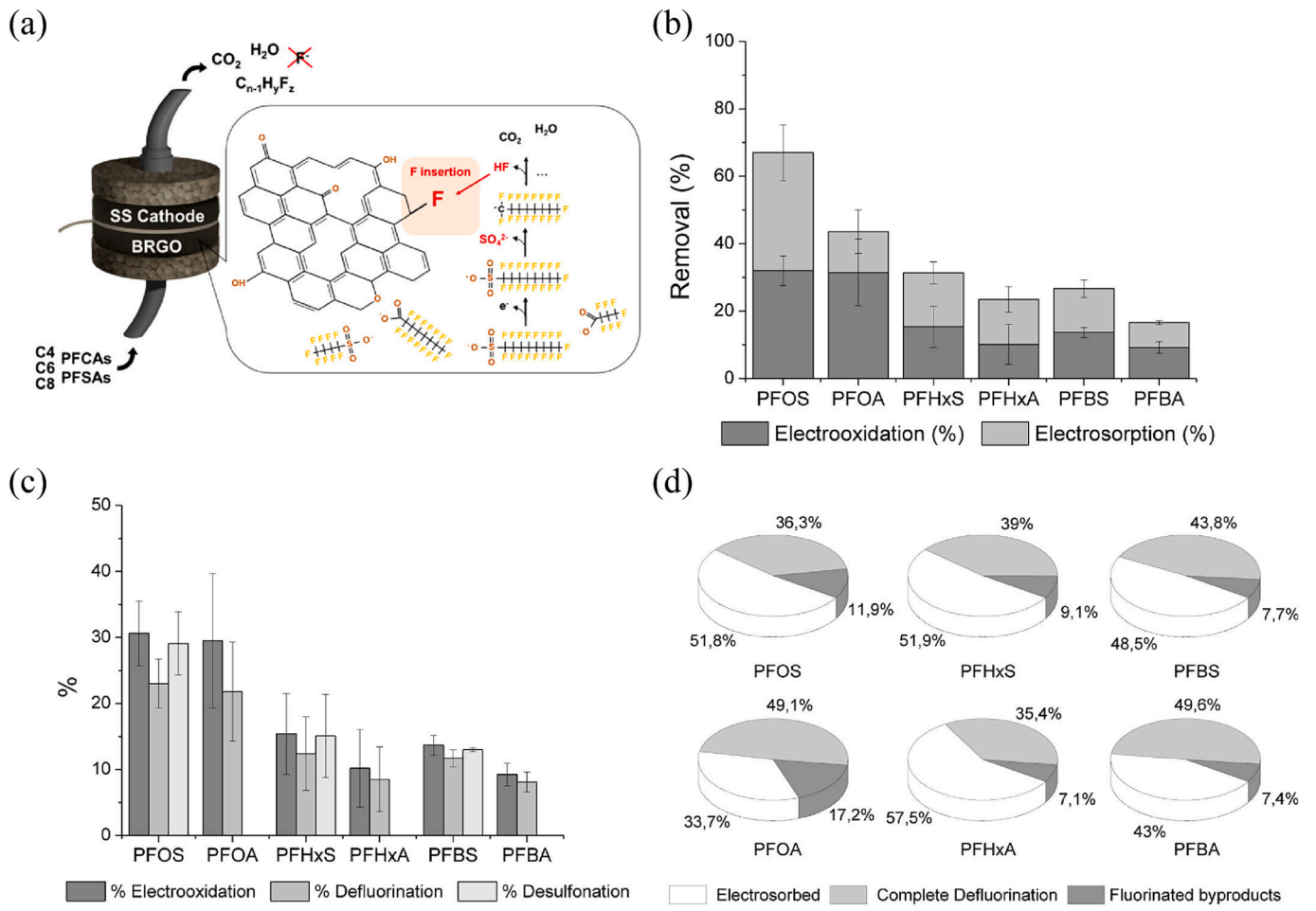

Fig. 11. (a) Illustration of the experiment with graphene sponge anode; (b) Removal efficiency of different PFAS species, (c) Electrooxidation, defluorination and desulfonation of different PFAS; (d) Proportion of electrosorbed, complete defluorination and fluorinated by products in the overall removal of each PFAS [94]. . Reproduced with permission from [94]

chosen as the electrolyte. If chloride is used, Cl-mediated oxidation may occur, while when sulfate is used, persulfate may form at the inert anode [170]. As shown in Tables 2 and 3, Na_2SO_4 and $NaClO_4$ are the most common electrolytes for PFAS electrooxidation due to their low cost and high conductivity [171].

5. Mechanism of electrochemical oxidations of PFASs

The reaction pathway of the PFOS oxidation was first investigated at boron-doped diamond (BDD) electrodes [87]. The density functional theory (DFT) model was used to investigate the activation barrier. The remediation of PFAS takes place through anodic oxidation (AO), in which hydroxyl radicals are generated at the surface of the anode during the EAOPs including regular electrochemical oxidation (EO), electro-fenton oxidation (EF), photoelectron-fenton oxidation (PEF), and sonoeletrochemistry (SE) [139]. These processes have been applied in the degradation of multiple man-made pollutants in wastewater and the remediation of industrial pollutants. The electrochemical decomposition mechanism for perfluorinated organic compounds (PFCs) by BDD electrode can be proposed by summarizing the experimental results from the previous literature [105] and further reproduced from the work of Brian P.Chaplin [3]. The degradation of PFOS is initiated by a direct electron transfer to the anode surface at a potential > 2.7 V/SHE [87]. The rate limiting step of PFASs oxidation is direct electron transfer concluded through a comparison of experimental and DET modelling analysis [3,87]. The reaction pathway shown in Fig. 13 incorporates both perfluorinated carboxylic acids and perfluorinated sulfonic acids. The PFC radicals formed by losing an electron to the anode then are converted to perfluoro radicals ($C_nF_{2n+1}^{\bullet}$). In Cycle I, $C_nF_{2n+1}^{\bullet}$ reacts with $OH^{\bullet}$ to produce $C_nF_{2n+1}O$ and H_2O, which then produce a CF_2O and $C_{n-1}F_{2n-1}^{\bullet}$. The cycle is repeated by the continuous generation of $OH^{\bullet}$ radicals, while significant short-chain by-products are produced. Cycle I has been identified from DFT model simulations with a total activation energy $<$ 35 kJ that is the most energetically favorable reaction pathway [172]. Other reaction mechanisms are proposed due to the detection of the low level of short-chained intermediates during the electrochemical oxidation of PFCs [87,88,140,141,150,173]. Cycle II is proposed in which $C_nF_{2n+1}^{\bullet}$ reacts with dissolved oxygen other than $OH^{\bullet}$ radicals and PFCs radicals to form $C_nF_{2n+1}O^{\bullet}$ and then yields COF_2 and $C_{n-1}F_{2n-1}^{\bullet}$. The COF_2 produced is further converted to CO_2 and HF with the participation of H_2O through hydrolysis. The cycle repeated producing progressively short-chained PFCs until complete mineralization occurs in Cycle III.

6. Challenges of electrochemical oxidation of PFASs

6.1. Slow reaction rate

EAOP of PFASs includes adsorption, electron transfer, bond breaking/formation and structural reorganization. Chemical or mass transportation processes limit the oxidation rate of pollutants. Furthermore, due to the strong bond of C–F and the unique structure of PFASs, their decomposition is relatively hard. In the EAOP of PFASs process, hydroxyl radicals are the main active components to decompose PFASs,

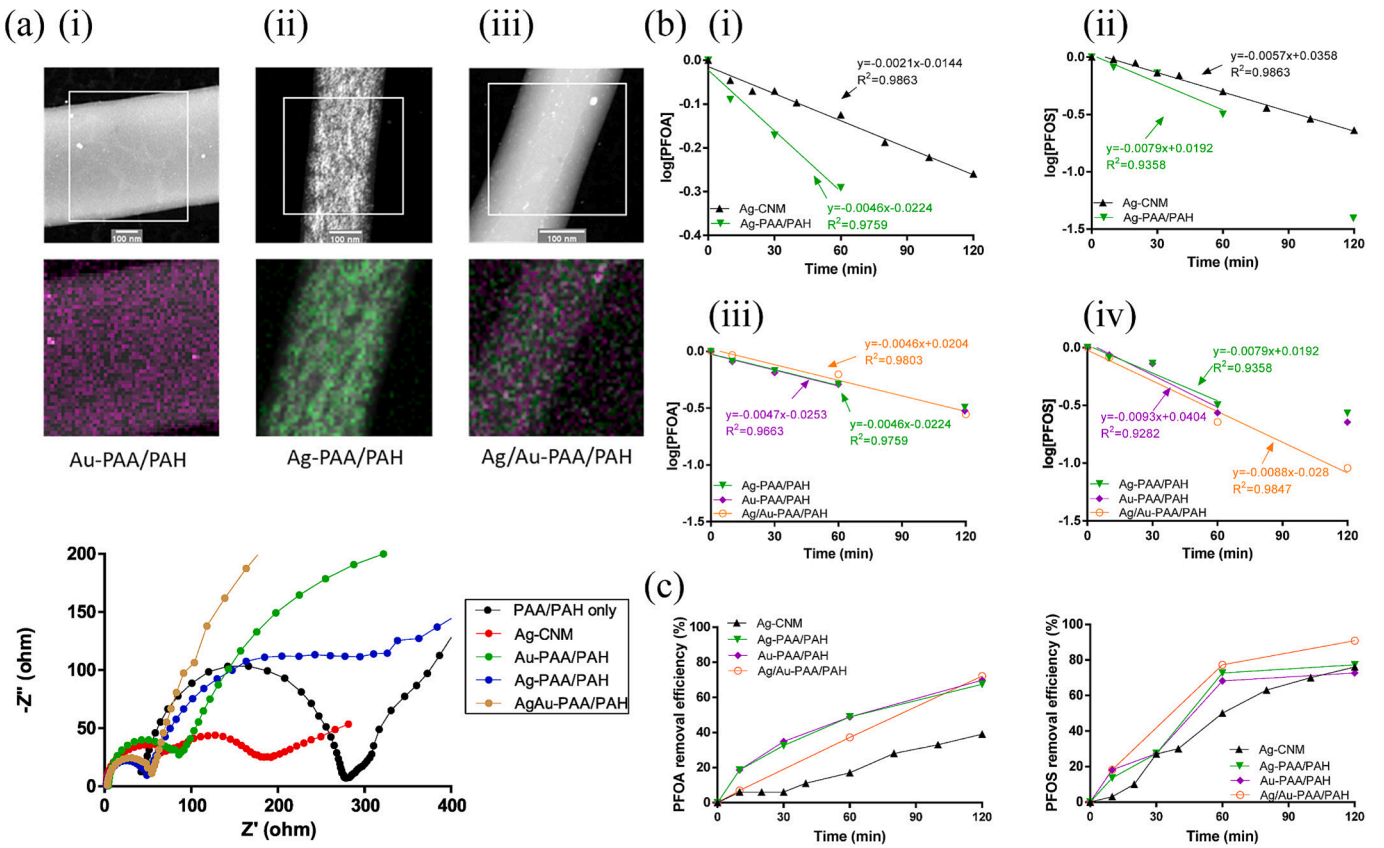

Fig. 12. (a) Images of NP-embedded hydrogel materials and impedance spectra with these different electrodes; (b) Removal rate of PFOA (i, iii) and PFOS (ii, iv) with different NP-embedded hydrogel materials; (c) Removal efficiency of PFOA (a) and PFOS (b) by different NP-embedded hydrogel materials [92]. .
Reproduced with permission from [92]

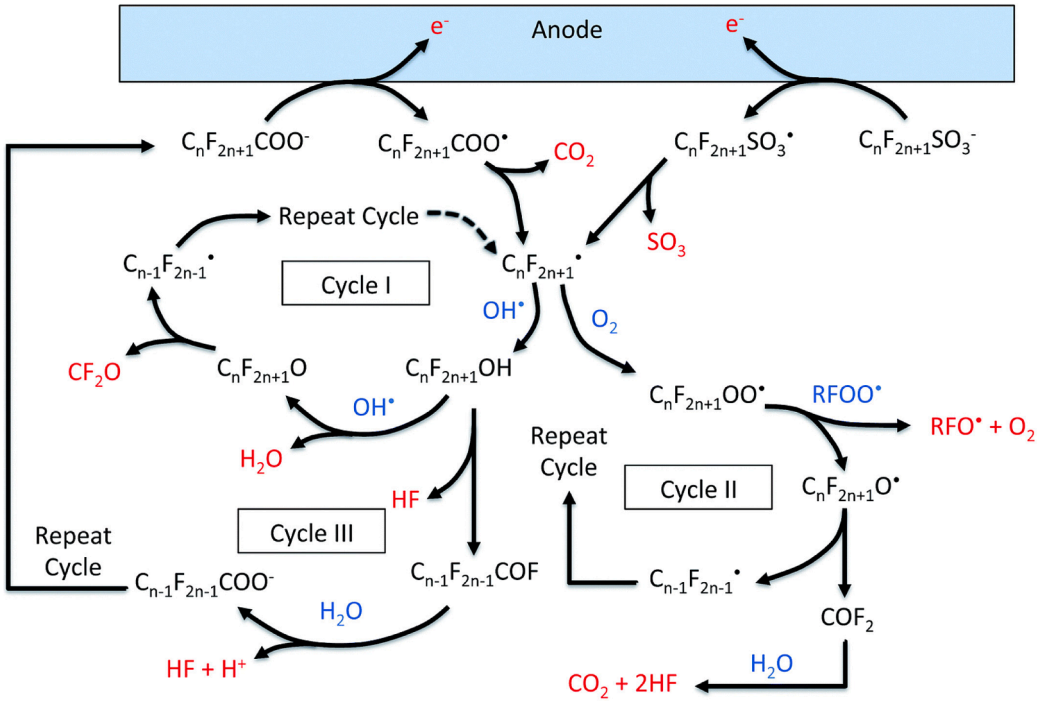

Fig. 13. Proposed electrochemical oxidation Mechanism of PFASs [3]. Reproduced with permission [3].

however, hydroxyl radicals produced by electrochemistry only exist on the surface of the anode because the lifetime of hydroxyl radicals is relatively short of only 2 ~ 4 μs. All these conditions lead to a slow reaction rate, which could be improved by (1) using the porous anode to extend the reaction to the whole porous anode; (2) forcing the effluent to transfer through the porous anode; (3) using the Fenton reaction, thus, the reaction could be extended from the surface of the anode to the whole anode, even the whole anode chamber by the Fenton reaction.

6.2. Secondary contamination

Undesired side reactions are inevitable due to the extremely high overpotential of hydroxyl radicals. Some by-products might be the source of secondary contamination, such as the production of chlorine and the formation of chlorate and perchlorate. Furthermore, the chemical process for EAOP decomposition of PFAS is complicated. The degradation reaction is mainly a series of carbon chain shortening reactions involving initial and subsequent steps and intermediates are inevitably generated during wastewater treatment. It is crucial to avoid and minimize toxic intermediates.

6.3. Long-term stability

Due to the strong C–F band, PFASs can only be degraded by "indirect electrolysis" at high anodic potential, where radicals with strong oxidizing and nonselective abilities are produced, such as hydroxyl ion •OH. Therefore, it is important to develop affordable, long-life electrodes for the process. While many materials exhibit cathodic stability, ensuring anodic stability remains a challenge [174]. Common anode electrodes for EPOA of PFAS include boron-doped diamond (BDD), Magnéli-phase Ti_4O_7, doped lead dioxide and doped SnO_2, which are stable at high overpotential because the process requires the active $OH^{\bullet}$. By contrast, electrode materials, such as graphite, graphene and perovskite are suitable for water splitting at low anodic overpotential. They do not generate $OH^{\bullet}$, and most of them are unstable under high anodic potential, so they are not effective for the long-term treatment of stubborn contaminants, such as PFAS.

7. Conclusions and perspectives

Since the introduction of PFAS in the 1940s, these compounds have been widely used due to their unique properties, especially their exceptional stability as surfactants. However, the remarkable stability of the carbon–fluorine bonds has also led to their bioaccumulation and widespread environmental presence. PFAS contamination has become a significant global issue, driving increased efforts to develop effective remediation strategies. Among the various methods explored for PFAS removal, EAOP has proven to be one of the most efficient. However, the commercialization of this technology faces challenges, such as slow reaction rates, potential secondary contamination, and the poor stability of electrodes. Additionally, no research has yet demonstrated complete defluorination of PFAS using EAOP. The full potential of the EAOP of PFASs can only be realized by addressing the following issues:

1. To better understand the mechanism of action of EAOP of PFASs on different types of anodic electrocatalysts, especially Magnéli phase titanium oxides.

Experimental and theoretical studies should be conducted to explore the potential reaction mechanisms using advanced in situ techniques such as in situ Raman spectroscopy, FTIR, DEMS, and in situ/near ambient pressure X-ray photoelectron spectroscopy (NAP-XPS). These methods provide powerful tools for identifying products and intermediates of electrochemical reactions, providing key insights into reaction pathways, product formation, and detailed monitoring of time-dependent electrocatalytic processes.

2. Better understanding of the fate of intermediates in the EAOP of PFASs process.

Although many studies have shown that EAOP can degrade up to 100 % of PFAS, complete defluorination via this method has not yet been reported. Therefore, further research is needed to better understand the fate of PFAS intermediates during the EAOP process. This could pave the way for the development of more advanced anode materials.

3. Reactor design

As mentioned earlier, the PFAS EAOP process involves adsorption, electron transfer, bond breaking/formation, and structural reorganization. However, the rate of pollutant oxidation may be limited by chemical or mass transfer processes. In addition, hydroxyl radicals, which play a key role in PFAS degradation, are only electrochemically generated at high overpotentials on specific metal oxide surfaces. To date, most studies have used small volumes of PFAS solutions, typically between 100 mL and 1000 mL. Therefore, designing larger-scale EAOP reactors is critical to achieving commercial feasibility.

4. Tandem EAOP of PFASs with other process.

Complete defluorination of PFAS by non-thermal technology is rare. Guan et al. [82] studied a photoelectrochemical process that fully exploited the hybrid advantages of PFAS photolysis and EAOP to achieve almost complete defluorination and mineralization of most PFAS. Recently, Luo et al. [175] investigated ultrasound-enhanced Ti_4O_7 electrochemical oxidation of PFOA. By combining ultrasound with EAOP, a significant improvement in the degradation of PFOA was observed. This synergistic effect was attributed to an activated and cleaned electrode surface, improved mass transfer, and enhanced production of reactive radicals.

In conclusion, EAOP for the degradation of PFASs holds great promise for commercialization. To fully realize this potential, both theoretical and experimental efforts are essential to develop novel, stable anode materials and to design advanced reactors. Additionally, combining EAOP with other processes—such as photolysis, and ultrasound—has shown promising results, further enhancing its effectiveness. Non-thermal plasma may offer another effective solution for PFAS degradation.

CRediT authorship contribution statement

Xiaoyong Xu: Writing – review & editing, Writing – original draft, Supervision, Methodology, Investigation, Funding acquisition, Conceptualization. **Yang Li:** Writing – original draft. **Phong H.N. Vo:** Writing – review & editing. **Pradeep Shukla:** Writing – review & editing. **Lei Ge:** Writing – review & editing. **Chun-Xia Zhao:** Writing – review & editing.

Declaration of competing interest

The authors declare that they have no known competing financial interests or personal relationships that could have appeared to influence the work reported in this paper.

Acknowledgement

X.X. acknowledges funding from the Australian Research Council (LP210301397).

Data availability

No data was used for the research described in the article.

References

[1] K.E. Pelch, A. Reade, C.F. Kwiatkowski, F.M. Merced-Nieves, H. Cavalier, K. Schultz, T. Wolffe, J. Varshavsky, The PFAS-Tox Database: a systematic evidence map of health studies on 29 per- and polyfluoroalkyl substances, Environ. Int. 167 (2022) 107408, https://doi.org/10.1016/j.envint.2022.107408.

[2] K. Prevedouros, I.T. Cousins, R.C. Buck, S.H. Korzeniowski, Sources, fate and transport of perfluorocarboxylates, Environ. Sci. Tech. 40 (1) (2006) 32–44, https://doi.org/10.1021/es0512475.

[3] B.P. Chaplin, Critical review of electrochemical advanced oxidation processes for water treatment applications, Environ. Sci.-Proc. Imp. 16 (6) (2014) 1182–1203, https://doi.org/10.1039/c3em00679d.

[4] K.H. Kucharzyk, R. Darlington, M. Benotti, R. Deeb, E. Hawley, Novel treatment technologies for PFAS compounds: a critical review, J. Environ. Manage. 204 (2017) 757–764.

[5] T.X.H. Le, H. Haflich, A.D. Shah, B.P. Chaplin, Energy-efficient electrochemical oxidation of perfluoroalkyl substances using a Ti4O7 reactive electrochemical membrane anode, Environ. Sci. Technol. Lett. 6 (8) (2019) 504–510, https://doi.org/10.1021/acs.estlett.9b00397.

[6] I. Ross, J. McDonough, J. Miles, P. Storch, P.T. Kochunarayanan, E. Kalve, J. Hurst, S.S. Dasgupta, J. Burdick, A review of emerging technologies for remediation of PFASs, Remediation 28 (2) (2018) 101–126, https://doi.org/10.1002/rem.21553.

[7] H. Hamid, L.Y. Li, J.R. Grace, Review of the fate and transformation of per- and polyfluoroalkyl substances (PFASs) in landfills, Environ. Pollut. 235 (2018) 74–84.

[8] W.J. Crinnion, The CDC fourth national report on human exposure to environmental chemicals: what it tells us about our toxic burden and how it assists environmental medicine physicians, Altern. Med. Rev. 15 (2) (2010) 101–108.

[9] J.P. Giesy, K. Kannan, Peer reviewed: perfluorochemical surfactants in the environment, Environ. Sci. Tech. 36 (7) (2002) 146A–A152, https://doi.org/10.1021/es022253t.

[10] Per- and Polyfluoroalkyl Substances (PFAS) Final PFAS National Primary Drinking Water Regulation, U.S. Environmental Protection Agency, 2024.

[11] J. Niu, Y. Li, E. Shang, Z. Xu, J. Liu, Electrochemical oxidation of perfluorinated compounds in water, Chemosphere 146 (2016) 526–538, https://doi.org/10.1016/j.chemosphere.2015.11.115.

[12] Y. Fujii, T. Niisoe, K.H. Harada, S. Uemoto, Y. Ogura, K. Takenaka, A. Koizum, Toxicokinetics of perfluoroalkyl carboxylic acids with different carbon chain lengths in mice and humans, J. Occup. Health 57 (1) (2015) 1–12, https://doi.org/10.1539/joh.14-0136-OA.

[13] H. Fromme, A. Dreyer, S. Dietrich, L. Fembacher, T. Lahrz, W. Voelkel, Neutral polyfluorinated compounds in indoor air in Germany – the LUPE 4 study, Chemosphere 139 (2015) 572–578, https://doi.org/10.1016/j.chemosphere.2015.07.024.

[14] S.J. Frisbee, A. Shankar, S.S. Knox, K. Steenland, D.A. Savitz, T. Fletcher, A. M. Ducatman, Perfluorooctanoic acid, perfluorooctanesulfonate, and serum lipids in children and adolescents, Arch. Pediatr. Adolesc. Med. 164 (9) (2010) 860–869.

[15] P. Favreau, C. Poncioni-Rothlisberger, B.J. Place, H. Bouchex-Bellomie, A. Weber, J. Tremp, J.A. Field, M. Kohler, Multianalyte profiling of per- and polyfluoroalkyl substances (PFASs) in liquid commercial products, Chemosphere 171 (2017) 491–501, https://doi.org/10.1016/j.chemosphere.2016.11.127.

[16] U. Eriksson, J.F. Mueller, L.-M.L. Toms, P. Hobson, A. Karrman, Temporal trends of PFSAs, PFCAs and selected precursors in Australian serum from 2002 to 2013, Environ. Pollut. 220 (2017) 168–177. doi: 10.1016/j.envpol.2016.09.036.

[17] K.T. Eriksen, M. Sorensen, J.K. McLaughlin, L. Lipworth, A. Tjonneland, K. Overvad, O. Raaschou-Nielsen, Perfluorooctanoate and Perfluorooctanesulfonate Plasma Levels and Risk of Cancer in the General Danish Population, Jnci-J. Natl. Cancer Inst. 101 (8) (2009) 605–609, https://doi.org/10.1093/jnci/djp041.

[18] E.A. Emmett, F.S. Shofer, H. Zhang, D. Freeman, C. Desai, L.M. Shaw, Community exposure to perfluorooctanoate: relationships between serum concentrations and exposure sources, J. Occup. Environ. Med. 48 (8) (2006) 759–770, https://doi.org/10.1097/01.jom.0000232486.07658.74.

[19] P.P. Egeghy, M. Lorber, An assessment of the exposure of Americans to perfluorooctane sulfonate: a comparison of estimated intake with values inferred from NHANES data, J. Expo Sci. Environ. Epid. 21 (2) (2011) 150–168, https://doi.org/10.1038/jes.2009.73.

[20] M.R. Earnshaw, A.G. Paul, R. Loos, S. Tavazzi, B. Paracchini, M. Scheringer, K. Hungerbuehler, K.C. Jones, A.J. Sweetman, Comparing measured and modelled PFOS concentrations in a UK freshwater catchment and estimating emission rates, Environ. Int. 70 (2014) 25–31, https://doi.org/10.1016/j.envint.2014.05.004.

[21] E.M. Sunderland, X.D.C. Hu, C. Dassuncao, A.K. Tokranov, C.C. Wagner, J. G. Allen, A review of the pathways of human exposure to poly- and perfluoroalkyl substances (PFASs) and present understanding of health effects, J. Expo Sci. Environ. Epid. 29 (2) (2019) 131–147, https://doi.org/10.1038/s41370-018-0094-1.

[22] V. Barry, A. Winquist, K. Steenland, Perfluorooctanoic acid (PFOA) exposures and incident cancers among adults living near a chemical plant, Environ. Health Persp. 121 (11–12) (2013) 1313–1318, https://doi.org/10.1289/ehp.1306615.

[23] J. Becanova, L. Melymuk, S. Vojta, K. Komprdova, J. Klanova, Screening for perfluoroalkyl acids in consumer products, building materials and wastes, Chemosphere 164 (2016) 322–329, https://doi.org/10.1016/j.chemosphere.2016.08.112.

[24] K. Hoffman, T.F. Webster, S.M. Bartell, M.G. Weisskopf, T. Fletcher, V.M. Vieira, Private drinking water wells as a source of exposure to perfluorooctanoic acid (PFOA) in communities surrounding a fluoropolymer production facility, Environ. Health Persp. 119 (1) (2011) 92–97, https://doi.org/10.1289/ehp.1002503.

[25] R. Vestergren, I.T. Cousins, Tracking the pathways of human exposure to perfluorocarboxylates, Environ. Sci. Tech. 43 (15) (2009) 5565–5575, https://doi.org/10.1021/es900228k.

[26] J.C. D'Eon, S.A. Mabury, Exploring indirect sources of human exposure to perfluoroalkyl carboxylates (PFCAs): evaluating uptake, elimination, and biotransformation of polyfluoroalkyl phosphate esters (PAPs) in the rat, Environ. Health. Persp. 119 (3) (2011) 344–350, https://doi.org/10.1289/ehp.1002409.

[27] C.H. Lindh, L. Rylander, G. Toft, A. Axmon, A. Rignell-Hydbom, A. Giwercman, H.S. Pedersen, K. Goalczyk, J.K. Ludwicki, V. Zvyezday, R. Vermeulen, V. Lenters, D. Heederik, J.P. Bonde, B.A.G. Jonsson, Blood serum concentrations of perfluorinated compounds in men from Greenlandic Inuit and European populations, Chemosphere 88 (11) (2012) 1269–1275, https://doi.org/10.1016/j.chemosphere.2012.03.049.

[28] V.M. Vieira, K. Hoffman, H.M. Shin, J.M. Weinberg, T.F. Webster, T. Fletcher, Perfluorooctanoic acid exposure and cancer outcomes in a contaminated community: a geographic analysis, Environ. Health Persp. 121 (3) (2013) 318–323, https://doi.org/10.1289/ehp.1205829.

[29] PFAS, Forever Chemicals Forecasted to Drive US$12.1 Billion in Water Utilities' Spend Over Next Decade, 2020. https://www.bluefieldresearch.com/ns/pfas-forever-chemicals/.

[30] D.Q. Zhang, W.L. Zhang, Y.N. Liang, Adsorption of perfluoroalkyl and polyfluoroalkyl substances (PFASs) from aqueous solution – a review, Sci. Total Environ. 694 (2019) 133606–133624, https://doi.org/10.1016/j.scitotenv.2019.133606.

[31] J. Qian, M. Shen, P. Wang, C. Wang, K. Li, J. Liu, B. Lu, X. Tian, Perfluorooctane sulfonate adsorption on powder activated carbon: effect of phosphate (P) competition, pH, and temperature, Chemosphere 182 (2017) 215–222, https://doi.org/10.1016/j.chemosphere.2017.05.033.

[32] J. Li, Q. Li, L.S. Li, L. Xu, Removal of perfluorooctanoic acid from water with economical mesoporous melamine-formaldehyde resin microsphere, Chem. Eng. J. 320 (2017) 501–509, https://doi.org/10.1016/j.cej.2017.03.073.

[33] D. Zhang, Q. Luo, B. Gao, S.Y.D. Chiang, D. Woodward, Q. Huang, Sorption of perfluorooctanoic acid, perfluorooctane sulfonate and perfluoroheptanoic acid on granular activated carbon, Chemosphere 144 (2016) 2336–2342, https://doi.org/10.1016/j.chemosphere.2015.10.124.

[34] Y. Zhi, J. Liu, Adsorption of perfluoroalkyl acids by carbonaceous adsorbents: effect of carbon surface chemistry, Environ. Pollut. 202 (2015) 168–176, https://doi.org/10.1016/j.envpol.2015.03.019.

[35] Z. Du, S. Deng, Y. Chen, B. Wang, J. Huang, Y. Wang, G. Yu, Removal of perfluorinated carboxylates from washing wastewater of perfluorooctanesulfonyl fluoride using activated carbons and resins, J. Hazard. Mater. 286 (2015) 136–143, https://doi.org/10.1016/j.jhazmat.2014.12.037.

[36] Y. Yao, K. Volchek, C.E. Brown, A. Robinson, T. Obal, Comparative study on adsorption of perfluorooctane sulfonate (PFOS) and perfluorooctanoate (PFOA) by different adsorbents in water, Water Sci. Technol. 70 (12) (2014) 1983–1991, https://doi.org/10.2166/wst.2014.445.

[37] M.F. Rahman, S. Peldszus, W.B. Anderson, Behaviour and fate of perfluoroalkyl and polyfluoroalkyl substances (PFASs) in drinking water treatment: a review, Water Res. 50 (2014) 318–340, https://doi.org/10.1016/j.watres.2013.10.045.

[38] Z. Du, S. Deng, Y. Bei, Q. Huang, B. Wang, J. Huang, G. Yu, Adsorption behavior and mechanism of perfluorinated compounds on various adsorbents – a review, J. Hazard. Mater. 274 (2014) 443–454, https://doi.org/10.1016/j.jhazmat.2014.04.038.

[39] J. Yu, L. Lv, P. Lan, S. Zhang, B. Pan, W. Zhang, Effect of effluent organic matter on the adsorption of perfluorinated compounds onto activated carbon, J. Hazard. Mater. 225–226 (2012) 99–106, https://doi.org/10.1016/j.jhazmat.2012.04.073.

[40] X. Zhao, Y. Cai, F. Wu, Y. Pan, H. Liao, B. Xu, Determination of perfluorinated compounds in environmental water samples by high-performance liquid chromatography-electrospray tandem mass spectrometry using surfactant-coated Fe3O4 magnetic nanoparticles as adsorbents, Microchem. J. 98 (2) (2011) 207–214, https://doi.org/10.1016/j.microc.2011.01.011.

[41] S.T.M.L.D. Senevirathna, S. Tanaka, S. Fujii, C. Kunacheva, H. Harada, B.H.A.K. T. Ariyadasa, B.R. Shivakoti, Adsorption of perfluorooctane sulfonate (n-PFOS) onto non ion-exchange polymers and granular activated carbon: batch and column test, Desalination 260 (1–3) (2010) 29–33, https://doi.org/10.1016/j.desal.2010.05.005.

[42] Q. Yu, R. Zhang, S. Deng, J. Huang, G. Yu, Sorption of perfluorooctane sulfonate and perfluorooctanoate on activated carbons and resin: kinetic and isotherm study, Water Res. 43 (4) (2009) 1150–1158, https://doi.org/10.1016/j.watres.2008.12.001.

[43] J. Yu, J. Hu, S. Tanaka, S. Fujii, Perfluorooctane sulfonate (PFOS) and perfluorooctanoic acid (PFOA) in sewage treatment plants, Water Res. 43 (9) (2009) 2399–2408, https://doi.org/10.1016/j.watres.2009.03.009.

[44] V. Ochoa-Herrera, R. Sierra-Alvarez, Removal of perfluorinated surfactants by sorption onto granular activated carbon, zeolite and sludge, Chemosphere 72 (10) (2008) 1588–1593, https://doi.org/10.1016/j.chemosphere.2008.04.029.

[45] P.A. Quinlivan, L. Li, D.R.U. Knappe, Effects of activated carbon characteristics on the simultaneous adsorption of aqueous organic micropollutants and natural

organic matter, Water Res. 39 (8) (2005) 1663–1673, https://doi.org/10.1016/j.watres.2005.01.029.
[46] P. Podkościelny, A. Dabrowski, O.V. Marijuk, Heterogeneity of active carbons in adsorption of phenol aqueous solutions, Appl. Surf. Sci. 205 (1–4) (2002) 297–303, https://doi.org/10.1016/S0169-4332(02)01154-6.
[47] C. Namasivayam, D. Kavitha, Removal of Congo Red from water by adsorption onto activated carbon prepared from coir pith, an agricultural solid waste, Dyes Pigm. 54 (1) (2002) 47–58, https://doi.org/10.1016/S0143-7208(02)00025-6.
[48] Y. Gao, S. Deng, Z. Du, K. Liu, G. Yu, Adsorptive removal of emerging polyfluoroalky substances F-53B and PFOS by anion-exchange resin: a comparative study, J. Hazard. Mater. 323 (2017) 550–557, https://doi.org/10.1016/j.jhazmat.2016.04.069.
[49] A. Zaggia, L. Conte, L. Falletti, M. Fant, A. Chiorboli, Use of strong anion exchange resins for the removal of perfluoroalkylated substances from contaminated drinking water in batch and continuous pilot plants, Water Res. 91 (2016) 137–146, https://doi.org/10.1016/j.watres.2015.12.039.
[50] S. Deng, Q. Yu, J. Huang, G. Yu, Removal of perfluorooctane sulfonate from wastewater by anion exchange resins: effects of resin properties and solution chemistry, Water Res. 44 (18) (2010) 5188–5195, https://doi.org/10.1016/j.watres.2010.06.038.
[51] L. Zhao, J. Bian, Y. Zhang, L. Zhu, Z. Liu, Comparison of the sorption behaviors and mechanisms of perfluorosulfonates and perfluorocarboxylic acids on three kinds of clay minerals, Chemosphere 114 (2014) 51–58, https://doi.org/10.1016/j.chemosphere.2014.03.098.
[52] K. Shih, F. Wang, Adsorption behavior of perfluorochemicals (PFCs) on boehmite: influence of solution chemistry, Proc. Environ. Sci. 18 (2013) 106–113.
[53] F. Wang, C. Liu, K. Shih, Adsorption behavior of perfluorooctanesulfonate (PFOS) and perfluorooctanoate (PFOA) on boehmite, Chemosphere 89 (8) (2012) 1009–1014, https://doi.org/10.1016/j.chemosphere.2012.06.071.
[54] Q. Zhou, S. Deng, Q. Yu, Q. Zhang, G. Yu, J. Huang, H. He, Sorption of perfluorooctane sulfonate on organo-montmorillonites, Chemosphere 78 (6) (2010) 688–694, https://doi.org/10.1016/j.chemosphere.2009.12.005.
[55] C.Y. Tang, Q. Shiang Fu, D. Gao, C.S. Criddle, J.O. Leckie, Effect of solution chemistry on the adsorption of perfluorooctane sulfonate onto mineral surfaces, Water Res. 44 (8) (2010) 2654–2662, https://doi.org/10.1016/j.watres.2010.01.038.
[56] S. Deng, Q. Zhang, Y. Nie, H. Wei, B. Wang, J. Huang, G. Yu, B. Xing, Sorption mechanisms of perfluorinated compounds on carbon nanotubes, Environ. Pollut. 168 (2012) 138–144, https://doi.org/10.1016/j.envpol.2012.03.048.
[57] X. Li, H. Zhao, X. Quan, S. Chen, Y. Zhang, H. Yu, Adsorption of ionizable organic contaminants on multi-walled carbon nanotubes with different oxygen contents, J. Hazard. Mater. 186 (1) (2011) 407–415, https://doi.org/10.1016/j.jhazmat.2010.11.012.
[58] X. Li, S. Chen, X. Quan, Y. Zhang, Enhanced adsorption of PFOA and PFOS on multiwalled carbon nanotubes under electrochemical assistance, Environ. Sci. Tech. 45 (19) (2011) 8498–8505, https://doi.org/10.1021/es202026v.
[59] X. Chen, X. Xia, X. Wang, J. Qiao, H. Chen, A comparative study on sorption of perfluorooctane sulfonate (PFOS) by chars, ash and carbon nanotubes, Chemosphere 83 (10) (2011) 1313–1319, https://doi.org/10.1016/j.chemosphere.2011.04.018.
[60] K. Yang, B. Xing, Adsorption of organic compounds by carbon nanomaterials in aqueous phase: polanyi theory and its application, Chem. Rev. 110 (10) (2010) 5989–6008, https://doi.org/10.1021/cr100059s.
[61] H. Moriwaki, Y. Takagi, M. Tanaka, K. Tsuruho, K. Okitsu, Y. Maeda, Sonochemical decomposition of perfluorooctane sulfonate and perfluorooctanoic acid, Environ. Sci. Tech. 39 (9) (2005) 3388–3392, https://doi.org/10.1021/es040342v.
[62] P.R. Kulkarni, S.D. Richardson, B.N. Nzeribe, D.T. Adamson, S.S. Kalra, S. Mahendra, J. Blotevogel, A. Hanson, G. Dooley, S. Maraviov, J. Popovic, Field demonstration of a sonolysis reactor for treatment of PFAS-contaminated groundwater, J. Environ. Eng. 148 (11) (2022) 06022005, https://doi.org/10.1061/(ASCE)EE.1943-7870.0002064.
[63] U. Eriksson, P. Haglund, A. Kärrman, Contribution of precursor compounds to the release of per- and polyfluoroalkyl substances (PFASs) from waste water treatment plants (WWTPs), J. Environ. Sci. 61 (2017) 80.
[64] H. Hori, E. Hayakawa, H. Einaga, S. Kutsuna, K. Koike, T. Ibusuki, H. Kiatagawa, R. Arakawa, Decomposition of environmentally persistent perfluorooctanoic acid in water by photochemical approaches, Environ. Sci. Tech. 38 (22) (2004) 6118.
[65] J. Chen, P.Y. Zhang, J. Liu, Photodegradation of perfluorooctanoic acid by 185 nm vacuum ultraviolet light, J. Environ. Sci. 19 (4) (2007) 387.
[66] H. Hori, A. Yamamoto, K. Koike, S. Kutsuna, I. Osaka, R. Arakawa, Persulfate-induced photochemical decomposition of a fluorotelomer unsaturated carboxylic acid in water, Water Res. 41 (13) (2007) 2962–2968, https://doi.org/10.1016/j.watres.2007.02.033.
[67] T. Yamamoto, Y. Noma, S.-I. Sakai, Y. Shibata, Photodegradation of perfluorooctane sulfonate by UV irradiation in water and alkaline 2-propanol, Environ. Sci. Tech. 41 (16) (2007) 5660–5665, https://doi.org/10.1021/es0706504.
[68] Y. Qu, C. Zhang, F. Li, J. Chen, Q. Zhou, Photo-reductive defluorination of perfluorooctanoic acid in water, Water Res. 44 (9) (2010) 2939.
[69] Y. Wang, P. Zhang, Photocatalytic decomposition of perfluorooctanoic acid (PFOA) by TiO2 in the presence of oxalic acid, J. Hazard. Mater. 192 (3) (2011) 1869.
[70] X. Li, P. Zhang, L. Jin, T. Shao, Z. Li, J. Cao, Efficient photocatalytic decomposition of perfluorooctanoic acid by indium oxide and its mechanism, Environ. Sci. Tech. 46 (10) (2012) 5528.
[71] Z. Li, P. Zhang, T. Shao, X. Li, In_2O_3 nanoporous nanosphere: a highly efficient photocatalyst for decomposition of perfluorooctanoic acid, Appl. Catal. B 125 (2012) 350–357.
[72] L.F. da Silva, W. Avansi, J. Andrés, C. Ribeiro, M.L. Moreira, E. Longo, V. R. Mastelaro, Long-range and short-range structures of cube-like shape SrTiO3 powders: microwave-assisted hydrothermal synthesis and photocatalytic activity, PCCP 15 (29) (2013) 12386–12393, https://doi.org/10.1039/C3CP50643F.
[73] M. Ohno, M. Ito, R. Ohkura, E.R. Mino, T. Kose, T. Okuda, S. Nakai, K. Kawata, W. Nishijima, Photochemical decomposition of perfluorooctanoic acid mediated by iron in strongly acidic conditions, J. Hazard. Mater. 268 (2014) (2014) 150–155.
[74] Y. Qu, C.J. Zhang, P. Chen, Q. Zhou, W.X. Zhang, Effect of initial solution pH on photo-induced reductive decomposition of perfluorooctanoic acid, Chemosphere 107 (2014) 218–223.
[75] P. Attri, Y.H. Kim, D.H. Park, J.H. Park, Y.J. Hong, H.S. Uhm, K.-N. Kim, A. Fridman, E.H. Choi, Generation mechanism of hydroxyl radical species and its lifetime prediction during the plasma-initiated ultraviolet (UV) photolysis, Sci. Rep.-Uk 5 (1) (2015) 9332, https://doi.org/10.1038/srep09332.
[76] L. Li, Z. Pan, Y. Ling, J. Huang, X. Li, X. Wang, Efficient degradation of perfluorooctanoic acid (PFOA) by photocatalytic ozonation, Chem. Eng. J. 296 (2016) 329.
[77] L. Jin, P. Zhang, Photochemical decomposition of perfluorooctane sulfonate (PFOS) in an anoxic alkaline solution by 185 nm vacuum ultraviolet, Chem. Eng. J. 280 (2015) 241.
[78] J. Xue, X. Zhu, Y. Zhang, W. Wang, W. Xie, J. Zhou, J. Bao, Y. Luo, X. Gao, Y. Wang, L.-Y. Jang, S. Sun, C. Gao, Cover Picture: nature of conduction band tailing in hydrogenated titanium dioxide for photocatalytic hydrogen evolution (ChemCatChem 12/2016), ChemCatChem 8 (12) (2016) 1991, https://doi.org/10.1002/cctc.201600682.
[79] S. Wang, Q. Yang, F. Chen, J. Sun, K. Luo, F. Yao, X. Wang, D. Wang, X. Li, G. Zeng, Photocatalytic degradation of perfluorooctanoic acid and perfluorooctane sulfonate in water: a critical review, Chem. Eng. J. 328 (2017) 927.
[80] M.J. Bentel, Y. Yu, L. Xu, Z. Li, B.M. Wong, Y. Men, J. Liu, Defluorination of per- and polyfluoroalkyl substances (PFASs) with hydrated electrons: structural dependence and implications to PFAS remediation and management, Environ. Sci. Tech. 53 (7) (2019) 3718–3728.
[81] Y. Wen, Á. Rentería-Gómez, G.S. Day, M.F. Smith, T.-H. Yan, R.O.K. Ozdemir, O. Gutierrez, V.K. Sharma, X. Ma, H.-C. Zhou, Integrated photocatalytic reduction and oxidation of perfluorooctanoic acid by metal-organic frameworks: key insights into the degradation mechanisms, J. Am. Chem. Soc. 144 (26) (2022) 11840–11850, https://doi.org/10.1021/jacs.2c04341.
[82] Y. Guan, Z. Liu, N. Yang, S. Yang, L.E. Quispe-Cardenas, J. Liu, Y. Yang, Near-complete destruction of PFAS in aqueous film-forming foam by integrated photo-electrochemical processes, Nat. Water 2 (5) (2024) 443–452, https://doi.org/10.1038/s44221-024-00232-7.
[83] M.S. Samuel, M. Shang, J. Niu, Photocatalytic degradation of perfluoroalkyl substances in water by using a duo-functional tri-metallic-oxide hybrid catalyst, Chemosphere 293 (2022) 133568, https://doi.org/10.1016/j.chemosphere.2022.133568.
[84] C.E. Schaefer, C. Andaya, A. Burant, C.W. Condee, A. Urtiaga, T.J. Strathmann, C. P. Higgins, Electrochemical treatment of perfluorooctanoic acid and perfluorooctane sulfonate: insights into mechanisms and application to groundwater treatment, Chem. Eng. J. 317 (2017) 424–432.
[85] Q. Zhuo, Q. Xiang, H. Yi, Z. Zhang, B. Yang, K. Cui, X. Bing, Z. Xu, X. Liang, Q. Guo, R. Yang, Electrochemical oxidation of PFOA in aqueous solution using highly hydrophobic modified PbO2 electrodes, J. Electroanal. Chem. 801 (2017) 235–243, https://doi.org/10.1016/j.jelechem.2017.07.018.
[86] A.M. Zaky, B.P. Chaplin, Porous substoichiometric TiO_2 anodes as reactive electrochemical membranes for water treatment, Environ. Sci. Tech. 47 (12) (2013) 6554–6563.
[87] K.E. Carter, J. Farrell, Oxidative destruction of perfluorooctane sulfonate using boron-doped diamond film electrodes, Environ. Sci. Tech. 42 (16) (2008) 6111–6115.
[88] H. Lin, J. Niu, S. Ding, L. Zhang, Electrochemical degradation of perfluorooctanoic acid (PFOA) by Ti/SnO_2-Sb, Ti/SnO_2-Sb/PbO_2 and Ti/SnO_2-Sb/MnO_2 anodes, Water Res. 46 (7) (2012) 2281–2289.
[89] S. Sharma, N.P. Shetti, S. Basu, M.N. Nadagouda, T.M. Aminabhavi, Remediation of per- and polyfluoroalkyls (PFAS) via electrochemical methods, Chem. Eng. J. 430 (2022) 132895–132910, https://doi.org/10.1016/j.cej.2021.132895.
[90] A. Román Santiago, P. Baldaguez Medina, X. Su, Electrochemical remediation of perfluoroalkyl substances from water, Electrochim. Acta 403 (2022) 139635–139650, https://doi.org/10.1016/j.electacta.2021.139635.
[91] S. Liang, R. Mora, Q. Huang, R. Casson, Y. Wang, S. Woodard, H. Anderson, Field demonstration of coupling ion-exchange resin with electrochemical oxidation for enhanced treatment of per- and polyfluoroalkyl substances (PFAS) in groundwater, Chem. Eng. J. Adv. 9 (2022) 100216–100224, https://doi.org/10.1016/j.ceja.2021.100216.
[92] J.-H. Hwang, Y.Y. Li Sip, K.T. Kim, G. Han, K.L. Rodriguez, D.W. Fox, S. Afrin, A. Burnstine-Townley, L. Zhai, W.H. Lee, Nanoparticle-embedded hydrogel synthesized electrodes for electrochemical oxidation of perfluorooctanoic acid (PFOA) and perfluorooctanesulfonic acid (PFOS), Chemosphere 296 (2022) 134001–134024, https://doi.org/10.1016/j.chemosphere.2022.134001.
[93] A. Fenti, Y. Jin, A.J.H. Rhoades, G.P. Dooley, P. Iovino, S. Salvestrini, D. Musmarra, S. Mahendra, G.F. Peaslee, J. Blotevogel, Performance testing of

mesh anodes for in situ electrochemical oxidation of PFAS, Chem. Eng. J. Adv. 9 (2022) 100205–100214, https://doi.org/10.1016/j.ceja.2021.100205.
[94] N. Duinslaeger, J. Radjenovic, Electrochemical degradation of per- and polyfluoroalkyl substances (PFAS) using low-cost graphene sponge electrodes, Water Res. 213 (2022) 118148–118156, https://doi.org/10.1016/j.watres.2022.118148.
[95] J.N. Uwayezu, I. Carabante, T. Lejon, P. van Hees, P. Karlsson, P. Hollman, J. Kumpiene, Electrochemical degradation of per- and poly-fluoroalkyl substances using boron-doped diamond electrodes, J. Environ. Manage. 290 (2021) 112573–112583, https://doi.org/10.1016/j.jenvman.2021.112573.
[96] S. Sukeesan, N. Boontanon, S.K. Boontanon, Improved electrical driving current of electrochemical treatment of Per- and Polyfluoroalkyl Substances (PFAS) in water using Boron-Doped Diamond anode, Environ. Technol. Innov. 23 (2021) 101655–101664, https://doi.org/10.1016/j.eti.2021.101655.
[97] J.S. Ko, N.Q. Le, D.R. Schlesinger, D. Zhang, J.K. Johnson, Z. Xia, Novel niobium-doped titanium oxide towards electrochemical destruction of forever chemicals, Sci. Rep.-Uk 11 (1) (2021) 18020–18030, https://doi.org/10.1038/s41598-021-97596-7.
[98] M. Ensch, C.A. Rusinek, M.F. Becker, T. Schuelke, A combined current density technique for the electrochemical oxidation of perfluorooctanoic acid (PFOA) with boron-doped diamond, Water Environ. J. 35 (1) (2021) 158–165, https://doi.org/10.1111/wej.12616.
[99] L. Wang, J. Lu, L. Li, Y. Wang, Q. Huang, Effects of chloride on electrochemical degradation of perfluorooctanesulfonate by Magnéli phase Ti_4O_7 and boron doped diamond anodes, Water Res. 170 (2020) 115254–115262, https://doi.org/10.1016/j.watres.2019.115254.
[100] A. Soriano, C. Schaefer, A. Urtiaga, Enhanced treatment of perfluoroalkyl acids in groundwater by membrane separation and electrochemical oxidation, Chem. Eng. J. Adv. 4 (2020) 100042–100050, https://doi.org/10.1016/j.ceja.2020.100042.
[101] C.E. Schaefer, D. Tran, Y. Fang, Y.J. Choi, C.P. Higgins, T.J. Strathmann, Electrochemical treatment of poly- and perfluoroalkyl substances in brines, Environ. Sci. Water Res. Technol. 6 (10) (2020) 2704–2712, https://doi.org/10.1039/D0EW00377H.
[102] A. Phetrak, P. Westerhoff, S. Garcia-Segura, Low energy electrochemical oxidation efficiently oxidizes a common textile dye used in Thailand, J. Electroanal. Chem. 871 (2020) 114301–114308, https://doi.org/10.1016/j.jelechem.2020.114301.
[103] M. Ensch, E. Davis, G.D. Landis, V.Y. Maldonado, M.F. Becker, C.A. Rusinek, N. Rancis, T. Schuelke, Electrochemical destruction of per- and polyfluoroalkyl substances (PFAS) in complex solution matrices, ECS Meeting Abstracts MA2020-01(21) (2020) 1264–1275, https://doi.org/10.1149/MA2020-01211264mtgabs.
[104] K. Kim, P. Baldaguez Medina, J. Elbert, E. Kayiwa, R.D. Cusick, Y. Men, X. Su, Molecular tuning of redox-copolymers for selective electrochemical remediation, Adv. Funct. Mater. 30 (52) (2020) 2004635–2004644, https://doi.org/10.1002/adfm.202004635.
[105] Q. Zhuo, S. Deng, B. Yang, J. Huang, B. Wang, T. Zhang, G. Yu, Degradation of perfluorinated compounds on a boron-doped diamond electrode, Electrochim. Acta 77 (2012) 17–22.
[106] O. Scialdone, A. Galia, G. Filardo, Electrochemical incineration of 1,2-dichloroethane: effect of the electrode material, Electrochim. Acta 53 (24) (2008) 7220–7225.
[107] C.E. Schaefer, C. Andaya, A. Urtiaga, E.R. McKenzie, C.P. Higgins, Electrochemical treatment of perfluorooctanoic acid (PFOA) and perfluorooctane sulfonic acid (PFOS) in groundwater impacted by aqueous film forming foams (AFFFs), J. Hazard. Mater. 295 (2015) 170–175.
[108] Q. Zhuo, M. Luo, Q. Guo, G. Yu, S. Deng, Z. Xu, B. Yang, X. Liang, Electrochemical oxidation of environmentally persistent perfluorooctane sulfonate by a novel lead dioxide anode, Electrochim. Acta 213 (2016) 358–367.
[109] H. Lin, J. Niu, S. Liang, C. Wang, Y. Wang, F. Jin, Q. Luo, Q. Huang, Development of macroporous Magnéli phase Ti4O7 ceramic materials: as an efficient anode for mineralization of poly- and perfluoroalkyl substances, Chem. Eng. J. 354 (2018) 1058–1067, https://doi.org/10.1016/j.cej.2018.07.210.
[110] K. Zhang, J. Huang, G. Yu, Q. Zhang, S. Deng, B. Wang, Destruction of perfluorooctane sulfonate (PFOS) and perfluorooctanoic acid (PFOA) by ball milling, Environ. Sci. Tech. 47 (12) (2013) 6471–6477, https://doi.org/10.1021/es400346n.
[111] S.-H. Ma, M.-H. Wu, L. Tang, R. Sun, C. Zang, J.-J. Xiang, X.-X. Yang, X. Li, G. Xu, EB degradation of perfluorooctanoic acid and perfluorooctane sulfonate in aqueous solution, Nucl. Sci. Tech. 28 (9) (2017) 137–144, https://doi.org/10.1007/s41365-017-0278-8.
[112] L. Wang, B. Batchelor, S.D. Pillai, V.S.V. Botlaguduru, Electron beam treatment for potable water reuse: removal of bromate and perfluorooctanoic acid, Chem. Eng. J. 302 (2016) 58–68, https://doi.org/10.1016/j.cej.2016.05.034.
[113] S.D. Pillai, Introduction to electron-beam food irradiation, Chem. Eng. Prog. 112 (11) (2016) 36–44.
[114] M. Javaherian, Bench-scale VEG research & development study: Implementation memorandum for ex-situ thermal desorption of perfluoroalkyl compounds (PFCs) in soils, Technical Note (2017).
[115] R.K. Singh, S. Fernando, S.F. Baygi, N. Multari, S.M. Thagard, T.M. Holsen, Breakdown products from perfluorinated alkyl substances (PFAS) degradation in a plasma-based water treatment process, Environ. Sci. Tech. 53 (5) (2019) 2731–2738, https://doi.org/10.1021/acs.est.8b07031.
[116] K. Tachibana, N. Takeuchi, K. Yasuoka, Reaction process of perfluorooctanesulfonic acid (PFOS) decomposed by DC plasma generated in argon gas bubbles, IEEE Trans. Plasma Sci. 42 (3) (2014) 786–793, https://doi.org/10.1109/Tps.2014.2304520.
[117] T.J.S.C. Higgins, Hydrothermal Technologies for On-Site Destruction of Site Investigation Wastes Contaminated with Per- and Polyfluoroalkyl Substances (PFAS)-SERDP Project ER18-1501 SEPTEMBER 2020, pp. 1–89.
[118] C. Luo, S. Teng, J. Wang, H. Xi, Energy yield from wastewater by supercritical water oxidation process: experimental validation and simulation from the viewpoint of energy system, Energ. Convers. Manage. 299 (2024) 117876, https://doi.org/10.1016/j.enconman.2023.117876.
[119] C.C. Murray, H. Vatankhah, C.A. McDonough, A. Nickerson, T.T. Hedtke, T. Y. Cath, C.P. Higgins, C.L. Bellona, Removal of per- and polyfluoroalkyl substances using super-fine powder activated carbon and ceramic membrane filtration, J. Hazard. Mater. 366 (2019) 160–168, https://doi.org/10.1016/j.jhazmat.2018.11.050.
[120] J.K. Johnson, C.M. Hoffman, D.A. Smith, Z. Xia, Advanced filtration membranes for the removal of perfluoroalkyl species from water, ACS Omega 4 (5) (2019) 8001–8006, https://doi.org/10.1021/acsomega.9b00314.
[121] J. Kujawa, S. Cerneaux, W. Kujawski, Removal of hazardous volatile organic compounds from water by vacuum pervaporation with hydrophobic ceramic membranes, J. Membr. Sci. 474 (2015) 11–19, https://doi.org/10.1016/j.memsci.2014.08.054.
[122] J. Kujawa, S. Cerneaux, W. Kujawski, Investigation of the stability of metal oxide powders and ceramic membranes grafted by perfluoroalkylsilanes, Colloids Surf. A Physicochem. Eng. Asp. 443 (2014) 109–117, https://doi.org/10.1016/j.colsurfa.2013.10.059.
[123] J. Kujawa, W. Kujawski, S. Koter, K. Jarzynka, A. Rozicka, K. Bajda, S. Cerneaux, M. Persin, A. Larbot, Membrane distillation properties of TiO2 ceramic membranes modified by perfluoroalkylsilanes, Desalin. Water Treat. 51 (7–9) (2013) 1352–1361, https://doi.org/10.1080/19443994.2012.704976.
[124] C.Y. Tang, Q.S. Fu, A.P. Robertson, C.S. Criddle, J.O. Leckie, Use of reverse osmosis membranes to remove perfluorooctane sulfonate (PFOS) from semiconductor wastewater, Environ. Sci. Tech. 40 (23) (2006) 7343–7349, https://doi.org/10.1021/es060831q.
[125] D.J. Burns, P. Stevenson, P.J.C. Murphy, PFAS removal from groundwaters using surface-active foam fractionation, Remediat. J. 31 (4) (2021) 19–33, https://doi.org/10.1002/rem.21694.
[126] T. Buckley, X. Xu, V. Rudolph, M. Firouzi, P. Shukla, Review of foam fractionation as a water treatment technology, Sep. Sci. Technol. 57 (6) (2022) 929–958, https://doi.org/10.1080/01496395.2021.1946698.
[127] P.H.N. Vo, T. Buckley, X. Xu, T.M.H. Nguyen, V. Rudolph, P. Shukla, Foam fractionation of per- and polyfluoroalkyl substances (PFASs) in landfill leachate using different cosurfactants, Chemosphere 310 (2023) 136869–136875, https://doi.org/10.1016/j.chemosphere.2022.136869.
[128] C. Fang, M. Megharaj, R. Naidu, Electrochemical advanced oxidation processes (EAOP) to degrade per- and polyfluoroalkyl substances (PFASs), J. Adv. Oxid. Technol. 20 (2) (2017) 20170014–20170025, https://doi.org/10.1515/jaots-2017-0014.
[129] J. Radjenovic, N. Duinslaeger, S.S. Avval, B.P. Chaplin, Facing the challenge of poly- and perfluoroalkyl substances in water: is electrochemical oxidation the answer? Environ. Sci. Tech. 54 (23) (2020) 14815–14829, https://doi.org/10.1021/acs.est.0c06212.
[130] M. Veciana, J. Bräunig, A. Farhat, M.-L. Pype, S. Freguia, G. Carvalho, J. Keller, P. Ledezma, Electrochemical oxidation processes for PFAS removal from contaminated water and wastewater: fundamentals, gaps and opportunities towards practical implementation, J. Hazard. Mater. 434 (2022) 128886–128903, https://doi.org/10.1016/j.jhazmat.2022.128886.
[131] M.A. Sandoval, W. Calzadilla, J. Vidal, E. Brillas, R. Salazar-González, Contaminants of emerging concern: occurrence, analytical techniques, and removal with electrochemical advanced oxidation processes with special emphasis in Latin America, Environ. Pollut. 345 (2024) 123397, https://doi.org/10.1016/j.envpol.2024.123397.
[132] A. Urtiaga, P. Fernandez-Castro, P. Gomez, I. Ortiz, Remediation of wastewaters containing tetrahydrofuran. Study of the electrochemical mineralization on BDD electrodes, Chem. Eng. J. 239 (2014) 341–350, https://doi.org/10.1016/j.cej.2013.11.028.
[133] M. Panizza, G. Cerisola, Direct and mediated anodic oxidation of organic pollutants, Chem. Rev. 109 (12) (2009) 6541–6569, https://doi.org/10.1021/cr9001319.
[134] L. Wang, J. Lu, L. Li, Y. Wang, Q. Huang, Effects of chloride on electrochemical degradation of perfluorooctanesulfonate by Magnéli phase Ti4O7 and boron doped diamond anodes, Water Res. 170 (2020) 115254, https://doi.org/10.1016/j.watres.2019.115254.
[135] H. Shi, Y. Wang, C. Li, R. Pierce, S. Gao, Q. Huang, Degradation of perfluorooctanesulfonate by reactive electrochemical membrane composed of Magnéli phase titanium suboxide, Environ. Sci. Tech. 53 (24) (2019) 14528–14537, https://doi.org/10.1021/acs.est.9b04148.
[136] J. Xie, C. Zhang, T.D. Waite, Hydroxyl radicals in anodic oxidation systems: generation, identification and quantification, Water Res. 217 (2022) 118425, https://doi.org/10.1016/j.watres.2022.118425.
[137] C. Barrera-Diaz, P. Canizares, F.J. Fernandez, R. Natividad, M.A. Rodrigo, Electrochemical advanced oxidation processes: an overview of the current applications to actual industrial effluents, J. Mex. Chem. Soc. 58 (2014) 256–275.
[138] N. Merino, Y. Qu, R.A. Deeb, E.L. Hawley, M.R. Hoffmann, S. Mahendra, Degradation and removal methods for perfluoroalkyl and polyfluoroalkyl substances in water, Environ. Eng. Sci. 33 (9) (2016) 615–649, https://doi.org/10.1089/ees.2016.0233.
[139] I. Sires, E. Brillas, M.A. Oturan, M.A. Rodrigo, M. Panizza, Electrochemical advanced oxidation processes: today and tomorrow. A review, Environ. Sci.

Pollut. Res. 21 (14) (2014) 8336–8367, https://doi.org/10.1007/s11356-014-2783-1.
[140] T. Ochiai, Y. Iizuka, K. Nakata, T. Murakami, D.A. Tryk, A. Fujishima, Y. Koide, Y. Morito, Efficient electrochemical decomposition of perfluorocarboxylic acids by the use of a boron-doped diamond electrode, Diam. Relat. Mater. 20 (2) (2011) 64–67, https://doi.org/10.1016/j.diamond.2010.12.008.
[141] Q.F. Zhuo, J.B. Wang, J.F. Niu, B. Yang, Y. Yang, Electrochemical oxidation of perfluorooctane sulfonate (PFOS) substitute by modified boron doped diamond (BDD) anodes, Chem. Eng. J. 379 (2020), https://doi.org/10.1016/j.cej.2019.122280.
[142] A. Urtiaga, C. Fernandez-Gonzalez, S. Gomez-Lavin, I. Ortiz, Kinetics of the electrochemical mineralization of perfluorooctanoic acid on ultrananocrystalline boron doped conductive diamond electrodes, Chemosphere 129 (2015) 20–26, https://doi.org/10.1016/j.chemosphere.2014.05.090.
[143] B.P. Chaplin, I. Wyle, H.J. Zeng, J.A. Carlisle, J. Farrell, Characterization of the performance and failure mechanisms of boron-doped ultrananocrystalline diamond electrodes, J. Appl. Electrochem. 41 (11) (2011) 1329–1340, https://doi.org/10.1007/s10800-011-0351-7.
[144] S. Garcia-Segura, E. Vieira dos Santos, C.A. Martínez-Huitle, Role of sp^3/sp^2 ratio on the electrocatalytic properties of boron-doped diamond electrodes: a mini review, Electrochem. Commun. 59 (2015) 52–55, https://doi.org/10.1016/j.elecom.2015.07.002.
[145] K. Muzyka, J. Sun, T.H. Fereja, Y. Lan, W. Zhang, G. Xu, Boron-doped diamond: current progress and challenges in view of electroanalytical applications, Anal. Methods 11 (4) (2019) 397–414, https://doi.org/10.1039/C8AY02197J.
[146] J.H.T. Luong, K.B. Male, J.D. Glennon, Boron-doped diamond electrode: synthesis, characterization, functionalization and analytical applications, Analyst 134 (10) (2009) 1965–1979, https://doi.org/10.1039/B910206J.
[147] S.J. Smith, M. Lauria, L. Ahrens, P. McCleaf, P. Hollman, S. Bjälkefur Seroka, T. Hamers, H.P.H. Arp, K. Wiberg, Electrochemical oxidation for treatment of PFAS in contaminated water and fractionated foam—a pilot-scale study, ACS ES&T Water 3(4) (2023) 1201–1211. doi: 10.1021/acsestwater.2c00660.
[148] A.B. Nienhauser, M.S. Ersan, Z. Lin, F. Perreault, P. Westerhoff, S. Garcia-Segura, Boron-doped diamond electrodes degrade short- and long-chain per- and polyfluorinated alkyl substances in real industrial wastewaters, J. Environ. Chem. Eng. 10 (2) (2022) 107192–107199, https://doi.org/10.1016/j.jece.2022.107192.
[149] A.M. Trautmann, H. Schell, K.R. Schmidt, K.M. Mangold, A. Tiehm, Electrochemical degradation of perfluoroalkyl and polyfluoroalkyl substances (PFASs) in groundwater, Water Sci. Technol. 71 (10) (2015) 1569–1575, https://doi.org/10.2166/wst.2015.143.
[150] B.G. Ruiz, S. Gomez-Lavin, N. Diban, V. Boiteux, A. Colin, X. Dauchy, A. Urtiaga, Efficient electrochemical degradation of poly- and perfluoroalkyl substances (PFASs) from the effluents of an industrial wastewater treatment plant, Chem. Eng. J. 322 (2017) 196–204, https://doi.org/10.1016/j.cej.2017.04.040.
[151] H. Lin, J. Niu, J. Xu, H. Huang, D. Li, Z. Yue, C. Feng, Highly efficient and mild electrochemical mineralization of long-chain perfluorocarboxylic acids (C9–C10) by Ti/SnO_2–Sb–Ce, Ti/SnO_2–Sb/Ce–PbO_2, and Ti/BDD electrodes, Environ. Sci. Tech. 47 (22) (2013) 13039–13046, https://doi.org/10.1021/es4034414.
[152] F.C. Walsh, R.G.A. Wills, The continuing development of Magnéli phase titanium sub-oxides and Ebonex® electrodes, Electrochim. Acta 55 (22) (2010) 6342–6351, https://doi.org/10.1016/j.electacta.2010.05.011.
[153] J. Huang, X. Che, J. Xu, W. Zhao, F. Xu, F. Huang, A reverse slipping strategy for bulk-reduced TiO_{2-x} preparation from Magnéli phase Ti_4O_7, Inorg. Chem. Front. 7 (1) (2020) 212–220, https://doi.org/10.1039/C9QI01042D.
[154] Y. Wang, L. Li, Y. Wang, H. Shi, L. Wang, Q. Huang, Electrooxidation of perfluorooctanesulfonic acid on porous Magnéli phase titanium suboxide Anodes: impact of porous structure and composition, Chem. Eng. J. 431 (2022) 133929, https://doi.org/10.1016/j.cej.2021.133929.
[155] A.C.M. Padilha, H. Raebiger, A.R. Rocha, G.M. Dalpian, Charge storage in oxygen deficient phases of TiO_2: defect physics without defects, Sci. Rep.-Uk 6 (1) (2016) 28871–28877, https://doi.org/10.1038/srep28871.
[156] Y. Wang, R.D. Pierce, H. Shi, C. Li, Q. Huang, Electrochemical degradation of perfluoroalkyl acids by titanium suboxide anodes, Environ. Sci. Water Res. Technol. 6 (1) (2020) 144–152, https://doi.org/10.1039/C9EW00759H.
[157] H. Lin, J.F. Niu, S.T. Liang, C. Wang, Y.J. Wang, F.Y. Jin, Q. Luo, Q.G. Huang, Development of macroporous Magneli phase Ti4O7 ceramic materials: as an efficient anode for mineralization of poly- and perfluoroalkyl substances, Chem. Eng. J. 354 (2018) 1058–1067, https://doi.org/10.1016/j.cej.2018.07.210.
[158] S.T. Liang, R. Pierce, H. Lin, S.Y. Chiang, Q. Huang, Electrochemical oxidation of PFOA and PFOS in concentrated waste streams, Remediation 28 (2) (2018) 127–134, https://doi.org/10.1002/rem.21554.
[159] Q.C. Ma, L. Liu, W. Cui, R.F. Li, T.T. Song, Z.J. Cui, Electrochemical degradation of perfluorooctanoic acid (PFOA) by Yb-doped Ti/SnO2-Sb/PbO2 anodes and determination of the optimal conditions, RSC Adv. 5 (103) (2015) 84856–84864, https://doi.org/10.1039/c5ra14299g.
[160] W. Mindt, Electrical Properties of Electrodeposited PbO[sub 2] Films, J. Electrochem. Soc. 116 (8) (1969) 1076, https://doi.org/10.1149/1.2412217.
[161] J.P. Carr, N.A. Hampson, Lead dioxide electrode, Chem. Rev. 72 (6) (1972) 679–703, https://doi.org/10.1021/cr60280a003.
[162] U.B. Thomas, The electrical conductivity of lead dioxide, J. Electrochem. Soc. 94 (2) (1948) 42, https://doi.org/10.1149/1.2773823.
[163] X. Li, D. Pletcher, F.C. Walsh, Electrodeposited lead dioxide coatings, Chem. Soc. Rev. 40 (7) (2011) 3879–3894, https://doi.org/10.1039/C0CS00213E.
[164] H.M. Zeyada, M.M. Makhlouf, Role of annealing temperatures on structure polymorphism, linear and nonlinear optical properties of nanostructure lead dioxide thin films, Opt. Mater. 54 (2016) 181–189, https://doi.org/10.1016/j.optmat.2016.02.031.
[165] J. Niu, H. Lin, J. Xu, H. Wu, Y. Li, Electrochemical mineralization of perfluorocarboxylic acids (PFCAs) by Ce-doped modified porous nanocrystalline PbO2 film electrode, Environ. Sci. Tech. 46 (18) (2012) 10191–10198, https://doi.org/10.1021/es302148z.
[166] Z. Xu, Y. Yu, H. Liu, J. Niu, Highly efficient and stable Zr-doped nanocrystalline PbO2 electrode for mineralization of perfluorooctanoic acid in a sequential treatment system, Sci. Total Environ. 579 (2017) 1600–1607, https://doi.org/10.1016/j.scitotenv.2016.11.180.
[167] C. Fang, Z. Sobhani, J. Niu, R. Naidu, Removal of PFAS from aqueous solution using PbO_2 from lead-acid battery, Chemosphere 219 (2019) 36–44, https://doi.org/10.1016/j.chemosphere.2018.11.206.
[168] Z. Lou, J. Wang, S. Wang, Y. Xu, J. Wang, B. Liu, C. Yu, J. Yu, Strong hydrophobic affinity and enhanced •OH generation boost energy-efficient electrochemical destruction of perfluorooctanoic acid on robust ceramic/PbO_2-PTFE anode, Sep. Purif. Technol. 280 (2022) 119919–119931, https://doi.org/10.1016/j.seppur.2021.119919.
[169] Q. Zhuo, S. Deng, B. Yang, J. Huang, G. Yu, Efficient electrochemical oxidation of perfluorooctanoate using a Ti/SnO2-Sb-Bi anode, Environ. Sci. Tech. 45 (7) (2011) 2973–2979, https://doi.org/10.1021/es1024542.
[170] C.A. Martínez-Huitle, M.A. Rodrigo, I. Sirés, O. Scialdone, Single and coupled electrochemical processes and reactors for the abatement of organic water pollutants: a critical review, Chem. Rev. 115 (24) (2015) 13362–13407, https://doi.org/10.1021/acs.chemrev.5b00361.
[171] L. Tian, M. Zhu, L.-S. Zhang, L.-J. Zhou, J.-P. Fan, D.-S. Wu, J.-P. Zou, New insights on the role of NaCl electrolyte for degradation of organic pollutants in the system of electrocatalysis coupled with advanced oxidation processes, J. Environ. Chem. Eng. 10 (3) (2022) 107414, https://doi.org/10.1016/j.jece.2022.107414.
[172] J. Niu, H. Lin, C. Gong, X. Sun, Theoretical and experimental insights into the electrochemical mineralization mechanism of perfluorooctanoic acid, Environ. Sci. Tech. 47 (24) (2013) 14341–14349, https://doi.org/10.1021/es402987t.
[173] Y.X. Bao, S.S. Deng, X.S. Jiang, Y.X. Qu, Y. He, L.Q. Liu, Q.W. Chai, M. Mumtaz, J. Huang, G. Cagnetta, G. Yu, Degradation of PFOA substitute: GenX (HFPO-DA Ammonium Salt): oxidation with UV/persulfate or reduction with UV/sulfite? Environ. Sci. Tech. 52 (20) (2018) 11728–11734, https://doi.org/10.1021/acs.est.8b02172.
[174] B.P. Chaplin, The prospect of electrochemical technologies advancing worldwide water treatment, Acc. Chem. Res. 52 (3) (2019) 596–604.
[175] Y. Luo, A. Khoshyan, M. Al Amin, A. Nolan, F. Robinson, J. Fenstermacher, J. Niu, M. Megharaj, R. Naidu, C. Fang, Ultrasound-enhanced Magnéli phase Ti4O7 anodic oxidation of per- and polyfluoroalkyl substances (PFAS) towards remediation of aqueous film forming foams (AFFF), Sci. Total Environ. 862 (2023), https://doi.org/10.1016/j.scitotenv.2022.160836.